Metal 4-Alkylidene-4*H*-pyridin-1-ides and 2*H*-Imidazol-4-ones from Novel Highly *N*-(Pyridin-4-yl)methyl-Substituted Azomethines

Diana Hampe,[a] Wolfgang Günther,[a] Helmar Görls,[b] and Ernst Anders*[a]

Keywords: Metalated azomethines / Heterocumulene fixation / Carboxylation / DFT calculations

Novel azomethines **3** synthesized from 4-(aminomethyl)pyridine (**1**) and various ketones **2** exhibit a higher acidity of the Cα-protons compared with other 4-alkylpyridines like 4-benzylpyridine or 4-(tosylmethyl)pyridine. Therefore, they can easily be metalated to give a variety of specific anions **3(–)**, which deserve interest for further synthetic applications. Important properties of compounds **3** and their lithiated derivatives **4** (lithium 4*H*-pyridin-1-ides, synthesized by deprotonation of the α-CH_2 group in **3**) can be controlled by the carbonyl reactant **2**. These carbanions **3(–)** are remarkable intermediates regarding their NMR properties. Comparing the NMR spectra of the lithium 4*H*-pyridin-1-ides **4** with their parent azomethines **3** reveal very distinct changes in the chemical shifts from which important structural and electronic properties of the carbanions can be deduced. The observation of *E*/*Z* isomers in the case of **3c** and their mutual conversion at higher temperature inspire DFT calculations on the B3LYP/6-311++G(d,p) level of theory to get insight into the energetic demand of such isomerization processes. Moreover, calculations on the same level of theory were carried out on the model azomethine anion **5** and different monomeric lithium coordination isomers **6a**–**d**. Experimentally, two selected examples will exemplify the reactivity of 4*H*-pyridin-1-ide anions towards heterocumulenes. The 2-(pyridin-4-yl)acetate **7** obtained from the reaction of **4e** with carbon dioxide appears to be a CO_2 storage molecule as it easily releases CO_2 under protolysis conditions comparable with the vitamin B_6 reaction mode. Interesting five-membered heterocycles were isolated after reaction of **4** with isocyanates followed by hydrolysis and oxidation.

Introduction

Imines, azomethines or Schiff bases − synonyms for one and the same species − are condensation products of primary amines with aldehydes or ketones.[1,2] Since azomethines are known they were introduced in a wide range of chemistry.

Their great *synthetic* importance reflects in a broad application: as protecting group for the C=O double bond or the amine function, as chiral auxiliaries in asymmetric substitution reactions of amino acids,[3] as reagent for the quantitative transfer of aldimines into aza-enolates or the synthesis of primary and secondary amines by reduction of the C=N double bond,[4] as ligands for various metals and the use of the resulting complexes as catalysts (e.g. polymerization, epoxidation of alkenes).[5−10] Azomethine ylides are widely used as 1,3-dipoles in cycloaddition reactions with several multi-bond systems like alkenes, acetylenes or carbonyls to give a great variety of different 5-ring heterocycles.[11]

Further, in *biological processes* of the amino acid metabolism azomethines also play an important role as key intermediates (Scheme 1): In reactions mediated by the derivatives of the vitamin B_6 complex, the formation of imines from amino acids and pyridoxal or α-keto acids and pyridoxamine, respectively, is the precondition for build-up and decomposition of amino acids, α-keto acids and biogenic amines by transamination or decarboxylation.[12]

The 2-[(pyridin-4(1*H*)-ylidenemethyl)imino] moiety (bold in **II**, Scheme 1) − a 4-alkylidene-1,4-dihydropyridine system extended by an imino function at the Cα center − is proposed as conceivable intermediate which facilitates the rearrangement of the C=N bond of the aldimine (structure **I**, Scheme 1) to the ketimine (structure **III**, Scheme 1) and the other way round by abstraction of a proton in α or α′ position as well as the loss of carbon dioxide (not shown in Scheme 1; instead of a proton, CO_2 is abstracted then).

The 4-alkylidene-1,4-dihydropyridine system is an object of thorough investigations by our work group since a longer time. Simple 4-alkylpyridines like 4-CH_3-, 4-*i*Pr- or 4-Bn-pyridine as well as more functionalized derivatives like 4-halomethyl-, 4-Me_3SiCH_2- or 4-(RSO_2CH_2)-pyridines were subjected to *N*-alkylations, *N*-acylations, deprotonations and subsequent reactions with various electrophiles.[13a−13h] In connection with investigations of several group transfer reagents, *N*-acyl-4-alkylidene-1,4-dihydropyridines and *N*-

[a] Institut für Organische Chemie und Makromolekulare Chemie der Friedrich-Schiller-Universität,
Humboldtstrasse 10, 07743 Jena, Germany
[b] Institut für Anorganische und Analytische Chemie der Friedrich-Schiller-Universität,
Lessingstrasse 8, 07743 Jena, Germany
Fax: (internat.) +49-(0)3641-948212
E-mail: Ernst.Anders@uni-jena.de

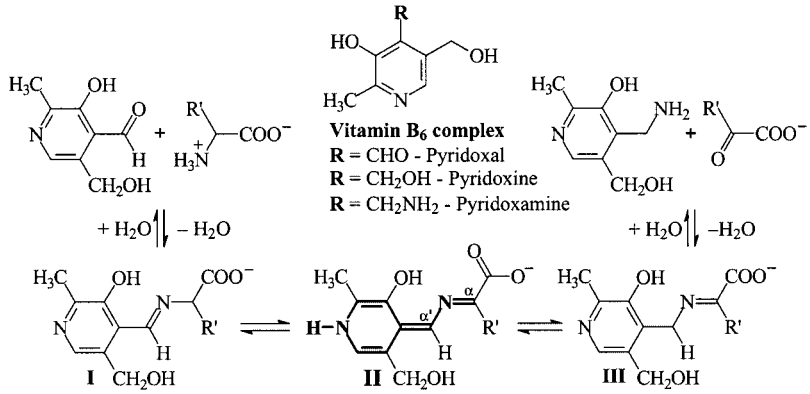

Scheme 1. 1,4-Dihydropyridine intermediate (bold, structure **II**) in the vitamin-B_6-catalyzed transamination reactions

acyl-4-alkylpyridinium salts emerge as useful tools in synthesis.[13i]

The interesting properties of the 1,4-dihydropyridine intermediates of amino acid aldimines in pyridoxal catalyzed reactions (Scheme 1) inspired us to investigate the chemistry of the related azomethines **3** from 4-(aminomethyl)pyridine (**1**) and the carbonyl compounds **2** as shown in Scheme 2 and 3. Moreover, the properties of the carbanions **3(−)** derived from **3**, especially, their potential ability to fixate and activate heterocumulenes, and their suitability to act as carbon dioxide transfer reagents in accordance to natural models like biotin or the above mentioned vitamin B6 will be part of this paper (Scheme 2 gives an impression of alternative reaction paths).

Furthermore, the introduction of the C=N double bond dilates the reaction diversity and opens the possibility to interesting cyclization reactions similar to 1,3-dipolar cycloadditions.

Structural and electronic backgrounds and explanations are given on the fundament of some high level DFT calculations which include the starting imines **3** − especially, their *Z*/*E* stereoisomerism − as their anions **3(−)** and lithiated counterparts **4** as well. They are summarized in the chapter *DFT calculations.*

A brief outlook should convey an insight into interesting reactivity properties of **4** towards heterocumulenes.

Results and Discussion

Azomethines

The synthesis of the azomethines **3** is a typical condensation reaction between 4-(aminomethyl)pyridine (**1**) and ketones **2** (Scheme 3) which tolerates a wide variety of substituents R^1 and R^2 of the carbonyl compounds **2**. Thus,

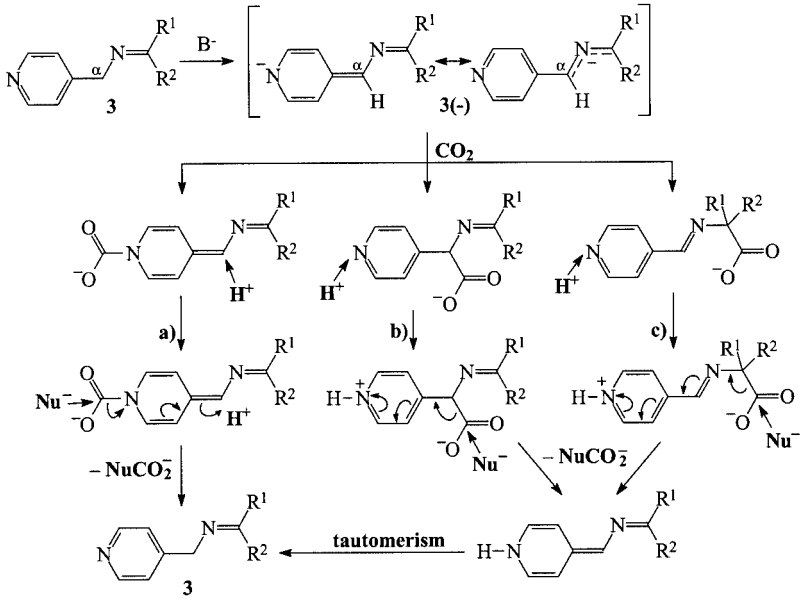

Scheme 2. Possible carbon dioxide adducts and their reaction modes as observed in natural processes. a) CO_2 transfer comparable with the biotin mode via a carbamate intermediate, b) Reaction mode resembling vitamin B_6 (to give the same intermediate as in **c**), c) Vitamin-B_6-like way of reaction

the reactivity and electronic properties of **3** and their carbanions **3(−)** can easily be adjusted to novel synthetic tasks (Scheme 3).

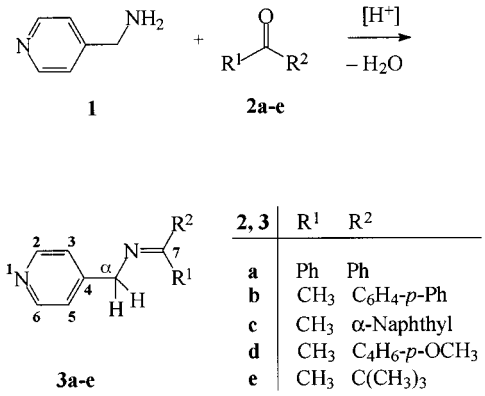

Scheme 3. Synthesis of azomethines **3** from 4-(aminomethyl)pyridine (**1**) and ketones **2**

From the standard procedure applied,[14] **3a**−**e** are obtained in yields between 50 and 65% as colorless or pale yellow crystal solids or powders.

With one exception (**2e**), the ketone reagents **2** carry at least one aromatic substituent as such moieties stabilize the C=N double bond due to conjugation with the aromatic π system.[2,14] Nevertheless, compounds **3** are in general sensitive towards moisture and show a distinct tendency for decomposition depending on the nature of R^1 and R^2 (cf. the Exp. Sect.). Therefore, it is recommended to store them under an inert gas atmosphere. Analogous aldimines **3** were not sufficiently stable. They polymerized to brown, highly viscous products.

E/*Z* Stereoisomerism

Due to the unsymmetrically substituted C=N double bond the imines **3b**−**e** can exist as *E*/*Z* stereoisomers. Interestingly, the appearance of these two isomers is only detectable for **3c** (Scheme 4) by NMR: Two signal sets (Table 1, Exp. Sect.) can be observed in ^1H and ^{13}C spectra in a ratio of about 83:17 (Figure 1). An equilibrium between the ketimine and its tautomeric aldimine in solution which differ from each by the position of the C=N double bond can be excluded because the ^1H NMR (Figure 1) shows neither a quadruplet for the methine proton nor a doublet of the corresponding methyl group (aldimine).

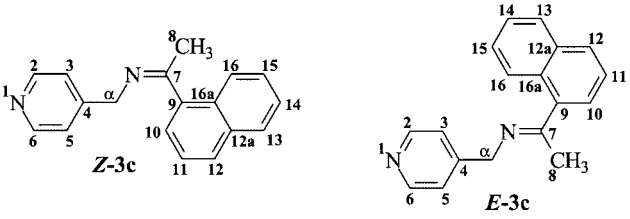

Scheme 4. *E*/*Z* isomers of **3c** (the numbering does not follow IUPAC rules, but should facilitate the description of the NMR results)

An in-depth structure determination was carried out by two dimensional NMR experiments (HMQC, HMBC, COSY, NOESY) in $CDCl_3$ at 0 °C. The exact configuration assignment could be realized by a two dimensional $^1H,^1H$ NOE spectroscopy (0 °C, $CDCl_3$). The interaction or noninteraction among the protons of the α-methylene and the methyl group is a reliable indicator for this differentiation: a cross signal will only appear for the *E* isomer. This NMR study showed, that the *E* isomer is present in much lower concentration (*Z*: 83%, *E*: 17%). This finding goes parallel with the result of our DFT calculations which predicted the *Z* isomer to be 2.1 kcal/mol more stable than the *E* isomer. Raising the temperature to 75 °C during the ^1H NMR measurement causes a change of the relative ratio from 83:17 to 60:40 as a thermally induced isomerization of the C=N bond takes place, presumably by inversion,[15,16] which additionally proves the coexistence of *E*/*Z* isomers. Further information concerning mechanism and activation energy was gained by DFT calculations (vide infra).

Comparing the chemical shifts of the α-methylene protons, protons H3/5 and H2/6 of both isomers of **3c** with those of the other imines **3a**,**b**−**e** (Table 1) indicates that the corresponding signals of ***Z*-3c** are shifted upfield while the signals of ***E*-3c** are in a similar range as the other imines. Furthermore, a clear tendency is recognizable for the chemical shift differences between the protons Hα, H3/5 and H2/6 of ***Z*-3c** and ***E*-3c**: the difference becomes smaller with greater spatial distance from the naphthyl substituent − $\Delta\delta$ = 0.6 ppm, 0.28 ppm and 0.1 ppm, respectively, i.e., the naphthyl residue causes a slight shielding of these protons in ***Z*-3c**. Thus, the 4-pyridylmethyl moiety must be orientated above or beneath the naphthyl ring plane so that the protons Hα, H3/5, H2/6 are affected by the ring current in decreasing strength with increasing distance. A further hint on the three-dimensional arrangement gives the NOESY spectrum where crosspeaks exist between the methyl group and the protons H10 and H16, respectively. Hence, the aromatic π system of the naphthyl substituent cannot be in the same plane with the π bond of the C=N double bond (otherwise only one crosspeak would be observable). Both these presumptions are confirmed by an X-ray crystal structure analysis of the *Z* isomer of **3c** (Figure 2).

The dihedral angle for imine-N (Nim), C7, C9 and C10 amounts to −96.1°, i.e., the C=N double bond does not profit from the stabilizing effect of the conjugation with the π system of the naphthyl residue. The planes spanned by Cα, Nim, C7 and Nim, C7, C8, respectively, enclose an dihedral angle of 178.2°, so these atoms almost lie in one plane. The dihedral angle between the pyridine ring and the C4−Cα−Nim plane is 61.7°. The naphthyl and pyridine rings are situated on opposite sides of the C=N plane and point away from each other so that they have the largest possible distance. Thus, the α-H atoms have different chemical surroundings. Therefore, the ^1H NMR signal of the diastereotopic α-methylene protons splits into four lines of an AB system (Figure 1). Another interesting observation is a

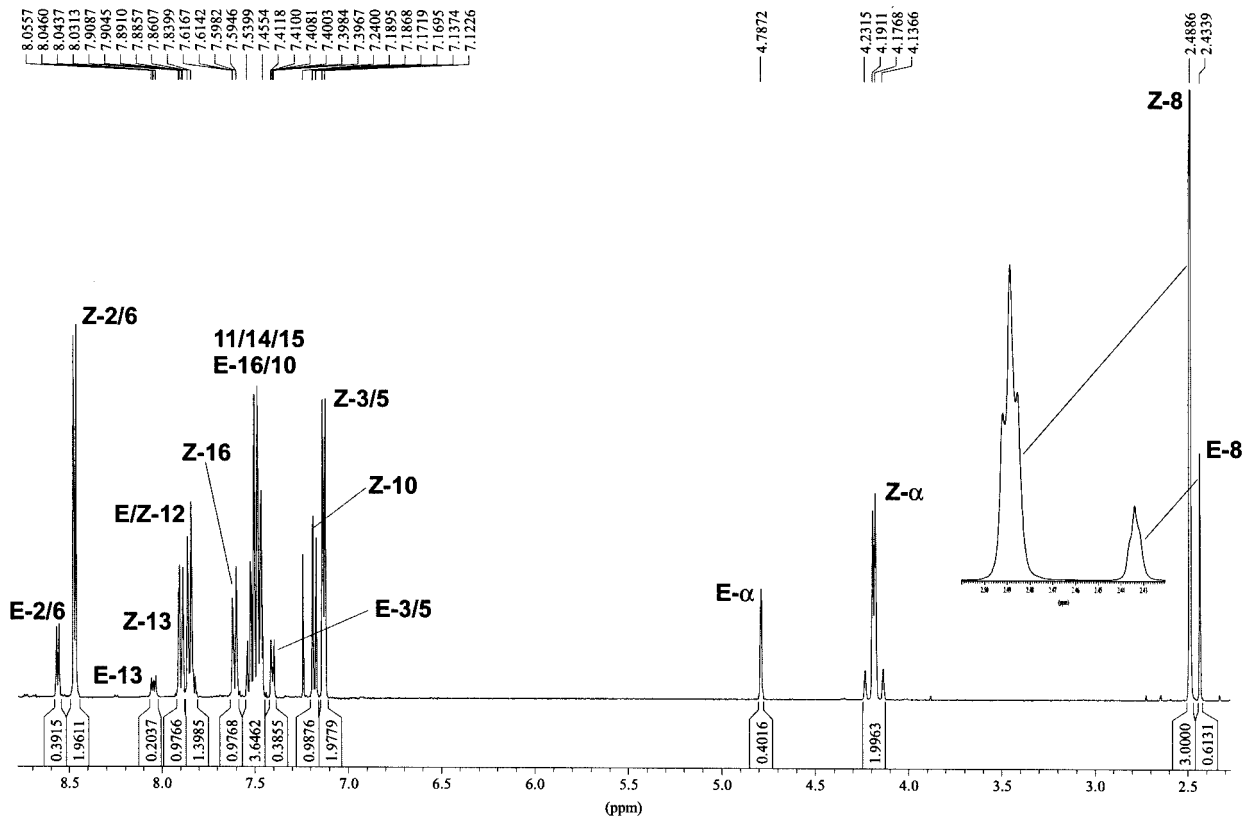

Figure 1. ^{1}H NMR of ***E/Z*-3c** measured at 400 MHz in $CDCl_3$ at 0 °C; the CH_3 groups are split into triplets because of a homoallyl coupling to the α-CH_2 group

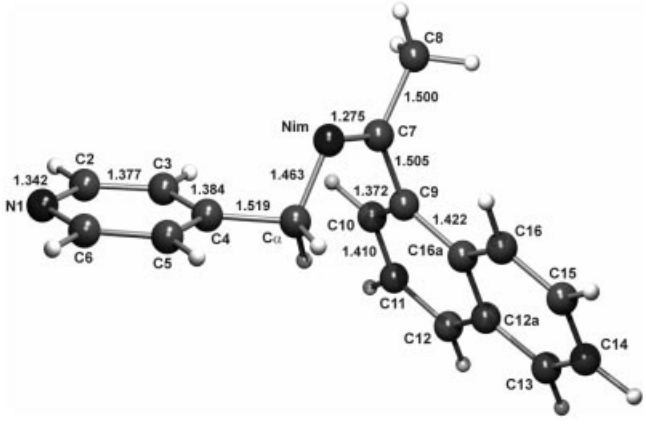

Figure 2. Molecular structure of ***Z*-3c** with selected bond lengths

homoallyl coupling between the α-CH_2 and CH_3 group of both isomers ***E/Z*-3c**. The CH_3 signals split into triplets with a small coupling constant of ^5J = 1.28 Hz for ***Z*-3c** and ^5J = 0.7−0.8 Hz for ***E*-3c**, respectively (Figure 1, enlargement of both triplets). This homoallyl coupling has also been observed for the CH_3 signal of **3b** (^5J = 0.78 Hz).

Interestingly, in the case of the other unsymmetrically substituted imines **3b**,**d**,**e** the NMR spectra show only one signal set what can be explained by formation of only one isomer in the synthesis, or a fast isomerization in regard to the NMR relaxation time takes place. But NOESY experiments reveal only crosspeaks between CH_2 and CH_3 group for all three imines **3b**,**d**,**e**. Thus, they exist in the *E* configuration.

Metalation of the Azomethines

Treatment of the azomethines **3** with various strong bases like metal organyls (*n*BuLi, $MgEt_2$), metal amides [LDA, $KN(SiMe_3)_2$] or alkoxides (KO*t*Bu) results in the metalated structures (M = Li: **4a**−**e**) after deprotonation of the α-methylene group (Scheme 5) in yields up to 95% depending on the metalating reagent.

The negative charge is strongly delocalized but of the many possible mesomeric structures Scheme 5 shows only those which mainly contribute to the resonance hybrid: The 4-alkylidene-1,4-dihydropyridine **A** from which the major participation is assumed, the 2-aza-allyl anion **B** in which the former positively polarized imine carbon is partially negatively charged, and a 4-alkylidene-3,4-dihydropyridine **C** which can be deduced from the calculated charge distributions of ***E*-3c(−)** and **5** (vide infra, Table 5, 9) as C3 and C5 bear a considerable negative partial charge of −0.28 (cf. the chapter DFT calculations). Of course, the effect of the metal coordination on the electron distribution should not be neglected (vide infra).

The substantially higher acidity of the α-methylene hydrogen atoms in comparison with that of the methyl hydrogen atoms in the azomethines **3b**−**d** (i.e. $R^1 = CH_3$) follows our expectation as in the anions resulting from the Cα de-

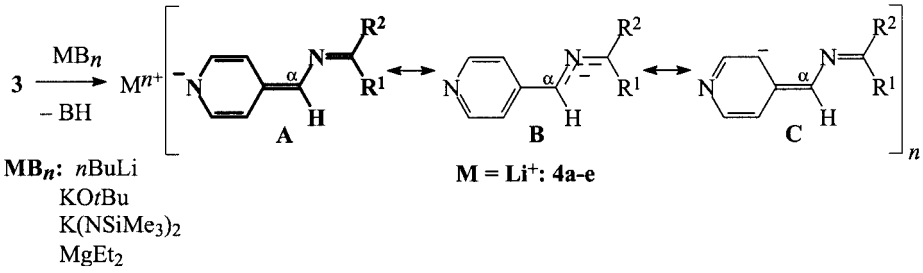

Scheme 5. Deprotonation of the 4-[(dialkylmethylenamino)methyl]pyridines **3** in Cα position (coordination modes of the metal cations are not considered)

protonation the charge is extremely well stabilized. If R^1 and/or R^2 are aryl residues they additionally can extend the conjugated system in the anions **3(−)**.

While KO*t*Bu, KN(SiMe$_3$)$_2$ or LDA are sterically demanding and therefore non-nucleophilic bases, the metal organyls *n*BuLi and MgEt$_2$ could act as nucleophiles and transfer an alkyl residue onto the C=N double bond or alkylate the pyridine ring in the 2-position. Fortunately, these reactions have not been observed under the applied reaction conditions. No deprotonation of the Cα atom was observed with ZnEt$_2$ in contrary to *n*BuLi and MgEt$_2$ what can be correlated to the more ionic metal−carbon bond in lithium and magnesium organyls and thus the more basic alkyl residues.[17] Moreover, no alkylation of the C=N double bond takes place with ZnEt$_2$.

Depending on the residues R^1 and R^2, the compounds **4a−e** are intensively colored: deep red (**4e**), deep magenta (**4a**,**d**) and deep blue violet (**4b**,**c**). The influence of the metal cation on the color of the carbanions **3(−)** is only small; the color of the corresponding potassium and magnesium compounds is similar to that of the lithium complexes **4**. The potassium compounds **K3(−)** were mainly synthesized by deprotonation with KN(SiMe$_3$)$_2$ in diethyl ether, but the use of KH or KO*t*Bu is also possible. The magnesium compounds **Mg[3(−)]$_2$** are accessible with MgEt$_2$ (THF, −20 °C). As selected examples **K3c(−)** and **Mg[3c(−)]$_2$** are given in the Exp. Sect.

As expected, all described metalated compounds **M[3(−)]$_n$** are very sensitive to moisture and protic solvents, and must be handled exclusively under inert conditions.

The lithium complexes **4** are in fact interesting intermediates, but difficult to handle so that they can only satisfactorily be characterized by NMR spectroscopy. Their extreme moisture sensitivity complicates other analyzing techniques (elemental analysis, MS, IR).

Some conceivable structures are calculated at the B3LYP/6-311++G(d,p) level of theory, indicating, that the lithium cation can migrate without significant energy demand to different positions resulting in the structures **6a−d** (see *DFT calculations*, Figure 5). The most stable monomeric structure appears to be **6a** while in general the reactivity pattern in solution will be determined by dimers such as **[4e(THF)$_2$]$_2$** (Figure 4) so that the structural and electronic properties of the anion of the least stable isomer **6d** appears to be the best model to describe the reaction behavior of such lithiated ambident structures in solution.[18]

The common reaction pattern of the azomethine anions **3(−)** towards electrophiles (heterocumulenes, aldehydes, esters) is the attack on the Cα atom with or without subsequent reactions (cf. the chapter *Reaction with heterocumulenes*), which is in some contradictions with the calculated charge distribution of the anions ***E*-3c(−)** and **5**, and the lithium species **6a−d** (cf. chapter *DFT calculations*), where the pyridine nitrogen bears the main part of the charge (q_N: −0.49 to −0.88) in comparison to the Cα atom (q_C: −0.11 to −0.26). Nevertheless, the preceding formation of a weak bond between the pyridine nitrogen and the electrophilic center cannot be excluded as this path would lead to a high reactive group transfer reagent which then can perform the attack on the Cα atom.

NMR Investigations

By comparison of the NMR spectra of imines **3a−e** (Table 1) and the lithium compounds **4a−e** (Table 2) information were gained regarding the charge distribution in the

Table 1. ^{1}H and ^{13}C NMR spectroscopic data of the azomethines **3** ($CDCl_3$; **3a**,**b**,**d**,**e:** 250/62.5 MHz, room temp.; **3c:** 400/100 MHz, 0 °C)

3 [a]	**a**	**b**	***Z*-c**[b]	***E*-c**[b]	**d**	**e**
δ_H						
H2/6	8.52	8.57	8.47	8.57	8.59	8.53
H3/5	7.28	[c]	7.13	7.41	7.43	7.33
Hα	4.56	4.70	4.19	4.79	4.69	4.43
CH_3	–	2.35	2.49	2.43	2.32	1.86
δ_C						
C2/6	149.7	149.8	149.7	149.9	149.9	149.6
C3/5	122.7	122.8	122.9	123.0	122.8	122.5
C4	149.7	149.7	149.1	149.2	150.0	150.3
Cα	56.1	54.4	55.2	54.9	54.2	53.2
C7	170.2	166.6	171.6	170.8	166.2	177.6
CH_3	–	16.0	29.8	21.1	15.7	13.8

[a] For numbering of compounds **3** cf. Scheme 4.[b] Two signal sets emerge for the *E*/*Z* mixture. [c] The signal of H3/5 overlaps with the signals of the *meta* and *para* protons of the 4-phenyl substituent to a multiplet at δ = 7.34−7.47 ppm.

carbanions. The chemical shift changes for the residues R^1, R^2 of **4a**−**e** are not so significant as for the (methyleneamino)pyridine moiety, hence, only the corresponding ^1H and ^{13}C signals are listed in Table 1 and Table 2, respectively.

Table 2. ^1H and ^{13}C NMR spectroscopic data of the lithium 4*H*-pyridinides **4** ([D$_8$]THF; **4a**,**b**,**d**,**e**: 250/62.5 MHz, room temp.)

4[a]	**a**	**b**	**c**[b][c]	**d**	**e**
δ_H					
H2	[d]	[e]	7.07	6.96	6.73
H3	[d]	[e]	6.95	6.81	6.42
H5	5.73	6.02	5.99	5.79	5.52
H6	7.01	[e]	7.05	6.89	6.67
Hα	6.04	6.19	6.21	5.96	5.56
CH_3	−	2.02	2.22	1.93	1.66
δ_C					
C2	145.7	144.9	144.8	144.2	143.3
C3	111.7	110.6	109.8	109.4	107.4
C4	148.1	146.6	146.6	145.1	142.7
C5	113.5	112.9	112.4	111.6	109.1
C6	145.3	144.5	144.7	144.0	143.2
Cα	106.8	105.9	106.0	103.7	99.4
C7	130.4	123.6	126.7	125.2	138.4
CH_3	−	11.1	15.7	11.2	10.8

[a] For numbering of compounds **4** cf. Scheme 4.[b] Only the *E*-isomer is observable. [c] Measurement at 400/100 MHz ($^1H/^{13}C$) and 0 °C. [d] The signals of H2/3 overlap with proton signals of the phenyl substituent to a multiplet at 7.11−7.17 ppm. [e] The signals of H2, H3 and H6 are overlapped to a multiplet at 7.09−7.18 ppm.

Because of the pyridine ring rotation around the C4−Cα bond in the azomethines **3** the proton pairs H2/6 and H3/5 and the corresponding carbon atoms C2/6 and C3/5 are chemically equivalent and thus have the same chemical shift. The signals of H2/6 in the compounds **3** are very similar; the H3/5 signals of ***Z*-3c** are slightly upfield shifted versus the H3/5 signals of the other imines **3**. The above mentioned shielding of the α-H in ***Z*-3c** brings about an upfield shift. The ^1H methyl group shifts of **3b**−**d** are similar except for **3e**. In the ^1H NMR spectrum of **3e** an upfield shift is observed due to the second aliphatic substituent (*t*Bu). The ^{13}C signals of the pyridine ring and the Cα position are very akin within the compounds **3**. The imine carbon C7 of **3e** shows the greatest downfield shift followed by ***Z*-3e** because the stabilization effect from the conjugation with an aromatic π system is lacking, thus, the imine carbon is more positively polarized. The ^{13}C CH_3 signal of ***E*/*Z*-3c** are clearly downfield shifted. Presumably, they are deshielded by the ring current effect of the naphthyl residue.

The strong upfield shift of the protons H2, H3, H5 and H6 (Δδ of H2/6: 1.41−1.86 ppm, H3: 0.18−0.91 ppm, H5: 1.14−1.81 ppm) and the carbon atoms C2, C3, C5 and C6 (Δδ of C2/6: 3−7 ppm, C3: 9−15 ppm, C5: 7−13 ppm) in **4** compared with **3** demonstrates a great amount of negative charge delocalization into the pyridine ring which is in accordance with the major participation of mesomeric structure **A** in the resonance hybrid (Scheme 5). In contrast to the imines **3**, separated signals appears for the protons and

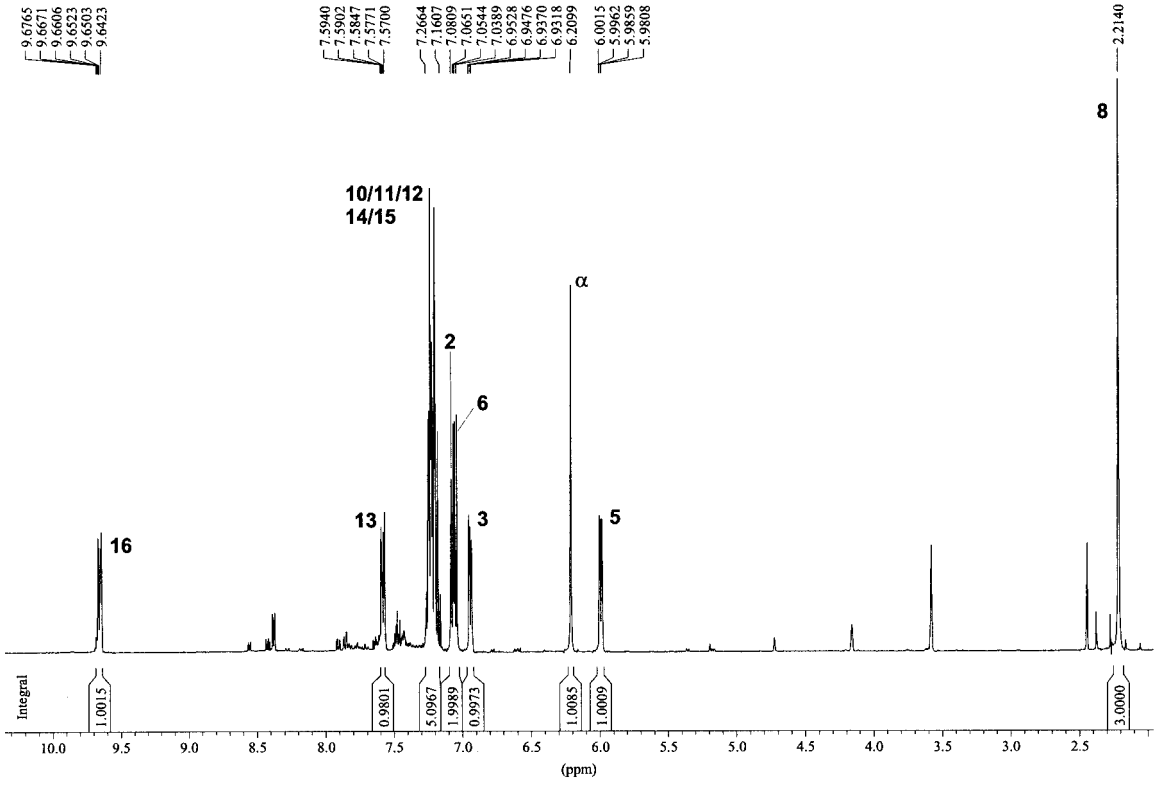

Figure 3. ^1H NMR of the lithium 4*H*-pyridin-1-ide **4c** ([D$_8$]THF, 0 °C, 400 MHz)

carbon atoms 2, 3, 5 and 6 as the rotation of the pyridine ring around the bond C4−Cα is no longer possible owing to its great double bond character. Thus, they have different chemical surroundings. While H3/5 and C3/5 are clearly separarted to ca. 1 ppm (^{1}H) and 2 ppm (^{13}C), H2/6 and C2/6 do not differ so much from each other: the doublets (^{1}H) are located closely abreast or appear as a triplet. The largest proton shift differences to the starting materials emerge for **4d** (Δδ: 1.62/1.69 ppm for H2/6, 0.6/1.81 ppm for H3/5) and **4e** (Δδ: 1.8/1.86 ppm for H2/6, 0.91/1.81 ppm for H3/5). In **4d** the 4-methoxy substituent enhances the electron density in the phenyl ring and, therefore, restricts the charge delocalization into the aromatic ring. In **4e** no aromatic substituent is available for charge distribution. Thus, the electron density in the 4-[(methyleneamino)methyl]pyridine moiety is higher in **4d**,**e** than in **4a**−**c**.

The C4 signals of the 4*H*-pyridinide in **4** are shifted upfield in the range of 1−7 ppm, whereat **4e** shows the largest difference in comparison with **3e**.

The Hα and Cα signals of **4** are shifted downfield by Δδ = 1.13−1.48 ppm (^{1}H) and 46−51 ppm (^{13}C) because of the change in carbon hybridization from sp^3 to sp^2 after deprotonation of **3**. In relation to other olefinic shift values (110−130 ppm), the Cα atoms experience a great amount of shielding due to the negative partial charge. In **4e**, the Cα atoms has the lowest value because no aromatic π system stabilizes the negative charge. With respect to the azomethines **3**, the imine carbon atoms C7 in **4** undergo the largest upfield shift of 39−44 ppm which is in good agreement with the mesomeric formula **B** of an 2-aza-allyl anion (Scheme 5). The above mentioned reason for the lower Cα shift value in **4e** compared to **4a**−**d** can be given for the higher C7 shifts in **4e** versus **4a**−**d**, too. But **4a** also shows a somewhat lower upfield shift compared to **4b**−**d**, because the phenyl rings cannot be localized in the same plane as the C=N double bond due to the repelling forces between the *ortho*-positioned hydrogen atoms. Hence, the delocalization into the aromatic substituents is reduced (i.e. less electron density is stabilized on C7). The H and C signals of the methyl groups in **4b**−**e** are slightly shielded compared to **3b**−**e** to about Δδ = 0.20−0.38 ppm (^{1}H) and 3−14 ppm (^{13}C) by the negative partial charge of the 2-aza-allyl anion. Compound **4c** shows the largest shift difference of 14.1 ppm.

A further interesting observation can be made for the lithium 4*H*-pyridin-1-ide **4c** which reveals a remarkable downfield shift of the naphthyl proton H16 from ca. 7.5/7.65 ppm in ***E*/*Z*-3c** to 9.65 ppm in **4c** (Figure 3). The NOESY spectrum displays crosspeaks of H16 to H3 and H2, but not to the methyl protons, thus, providing an evidence for the *E* configuration of **4c** (see Scheme 3). Possibly, a weak hydrogen bond exists between H16 and the imine-N (six-membered ring) or H16 reaches into the negative area of the anisotropy cone of the 2-aza-allyl system or the C=N double bond, respectively. On the B3LYP/6-311++G(d,p) theory level, the H16−Nim distance was determined to 2.202 Å (vide infra) which is very short for a hydrogen bond.[19] Therefore, the down field shift is supposed to be primarily attributed to the electronic influence of the 2-aza-allyl anion.

Finally, a structure motif of a dimer of **4e** is presented in Figure 4 to back up the results of the above described NMR investigations.

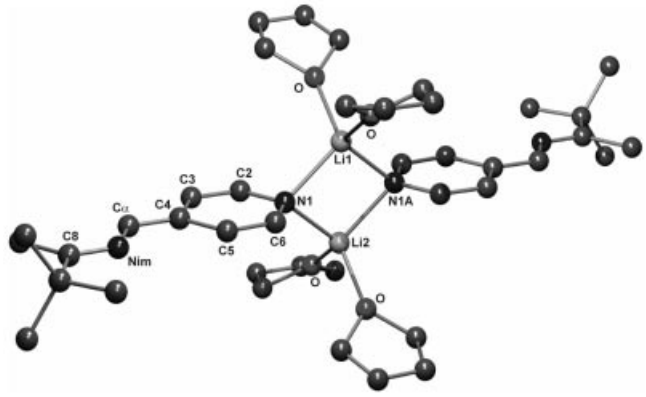

Figure 4. Structure motif of **[4e(THF)$_2$]$_2$** [33−37] − a dimer of **4e**

The 4*H*-pyridin-1-ide anion in **4e** is *E* configured regarding the C=N double bond. The lithium ions are coordinated by the N atoms of the 4*H*-pyridinide rings in an asymmetrically way and each by two solvent molecules (THF) in a tetrahedral mode.

Because of these results we conjecture that compounds **4b**,**d** also adopt *E* configuration, but in order to unambiguously prove it further NOESY measurements must be carried out.

DFT Calculations

***E*/*Z* Isomerization of 3c:** As mentioned above orientating DFT calculations on the B3LYP/6-311++G(d,p) level of theory using the GAUSSIAN 98 program package[20] were

Table 3. Absolute and relative energies for the calculated structures ***Z*-3c**, ***E*-3c** and the *E*/*Z* isomerization **TS**

Structure	abs. *E*[a] [a.u.]	ZPE [a.u.]	ZPE-corr. *E* [a.u.]	rel. *E* Δ*E* [kcal·mol^{-1}]	NIMAG[b]
***Z*-3e**	−805.250789	0.292666	−804.958123	0.0	[0]
***E*-3c**	−805.247460	0.292688	−804.954772	2.1	[0]
TS	−805.208817	0.290602	−804.918215	25.0	[1]

[a] B3LYP/6-311++G(d,p) optimizations. [b] *N*umber of *imag*inary frequencies

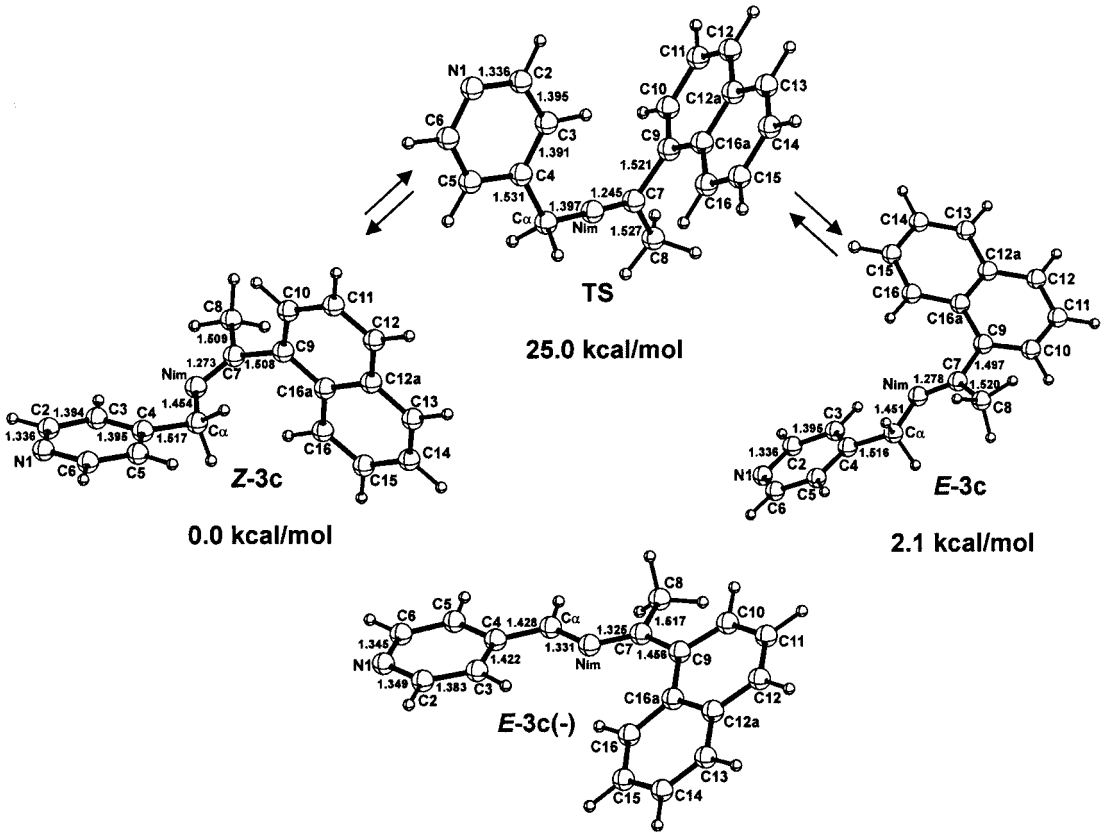

Scheme 6. Calculated structures of ***Z*-3c**, ***E*-3c**, and the **TS** for the *E*/*Z* isomerization: an *inversion mechanism* (B3LYP/6-311++G(d,p) results). For completeness, the structure of the *E*-configured anion of **3c(−)** is depicted, too

carried out to get insight into the isomerization mechanism of ***Z*/*E*-3c**. The calculated structures of ***Z*-3c**, ***E*-3c** and the transition state **TS** are depicted in Scheme 6. The crystal structure data were the starting point for the calculations (using the RES file as input). Bond lengths (in Å) of the molecular structure of ***Z*-3c** (Figure 2) and the calculated structures are listed in Table 4. Moreover, the anion of **3c** with *E* configuration (Scheme 6) was optimized on the same level of theory to perform an NBO[21] analysis. The charge distribution obtained is summarized in Table 5.

Table 4. Selected bond lengths (BL, in Å) of the crystal structure of ***Z*-3c** and the calculated structures of ***Z*-3c**, ***E*-3c**, the *E*-anion **3c(−)**, and the **TS** for the *E*/*Z* isomerization; the naphthyl bonds are omitted for clearness

Bond	Exp. BL	calcd. BL			
	***Z*-3c**[a]	***Z*-3c**[b]	***E*-3c**	**TS** (inversion)	***E*-3c(−)**
N1−C2	1.342 (3)	1.336	1.336	1.336	1.349
N1−C6	1.332 (3)	1.338	1.338	1.338	1.345
C2−C3	1.377 (4)	1.394	1.395	1.395	1.383
C3−C4	1.384 (3)	1.395	1.393	1.391	1.422
C4−C5	1.381 (3)	1.398	1.398	1.397	1.421
C5−C6	1.380 (3)	1.392	1.391	1.391	1.384
C4−Cα	1.519 (3)	1.517	1.516	1.531	1.428
Cα−Nim	1.463 (3)	1.454	1.451	1.397	1.331
Nim-C7	1.275 (3)	1.273	1.278	1.245	1.325
C7−C8	1.500 (4)	1.509	1.520	1.527	1.517
C7−C9	1.505 (3)	1.508	1.497	1.521	1.456

[a] Data taken from the crystal structure. [b] Calculated values.

Table 5. Charge distribution in the anion ***E*-3c(−)** (Scheme 6) as result from an NBO analysis (NBO version 3.0[21]) on the B3LYP/6-311++G(d,p) level of theory. Charges of the protons are omitted

Atom	Charge	Atom	Charge
N1	−0.55	Cα	−0.12
C2/6	0.03	Nim	−0.47
C3/5	−0.28		
C4	−0.03	C7	0.12

In general, two mechanisms can be discussed: a rotation about the C=N double bond or an inversion of the (pyridin-4-yl)methyl residue on the imine nitrogen, respectively.[15,16] A coupled mechanism with both inversional and torsional components must also be taken into account. The transition state **TS**, as simplified depicted in Scheme 6, is characterized by a linear arrangement of the Cα, Nim and C7 atoms (bond angle 180°). Both bonds Cα−Nim (1.394 Å) and Nim−C7 (1.245 Å) are shortened compared with ***Z*-3c** and ***E*-3c** (Table 4). Hence, the hybridization of the imine nitrogen ranges between sp^2 and sp. Thus, the isomerization mechanism can be denoted as an inversion. The bonds C7−C8 and C7−C9 are somewhat lengthened to avoid steric hindrance between the naphthyl and the methyl

group on C7. The pyridine ring almost lies in the Cα−Nim−C7−C8 plane, the naphthyl ring almost stands perpendicular on that plane (Scheme 6).

Surprisingly, the *Z*-isomer is about 2.1 kcal/mol more stable than its *E* counterpart. The energy barrier for their transformation (**TS**) is with 25.0 kcal/mol somewhat higher than for some experimentally investigated C=N double bond systems. Kessler et al. determined the free activation enthalpies for *E*/*Z* isomerizations of different 2,4,6-triisopropyl-substituted anils by inversion with ^{1}H NMR coalescence measurements of diastereotopic groups bound on the imine carbon. Their highest experimentally obtained value was 19.8 kcal/mol (coalescence temperature 102 °C).[15a] Marullo and Wagener determined the free activation energies of the azomethines derived from aceton and aniline and benzylamine, respectively, to 21 kcal/mol and > 23 kcal/mol by measurement of the coalescence temperature.[16c] Hofmann et al. calculated on the STO-3G level of theory values of 23−30 kcal/mol for the linear inversion transition state of three different anil types.[16d]

Comparing the crystal structure of ***Z*-3c** (Figure 2) with its calculated analogue (Scheme 6) the most striking difference is a conformational one. The imino moiety (torsion angle 61.7° in the crystal) is turned for 55.2° almost into the plane of the pyridine ring by rotation along the Cα−Nim bond (torsion angle 16.5°). That is certainly the result of packing effects in the solid state. Since the crystal structure data was chosen as input for the optimization the geometry of ***Z*-3c**, such a structure does not represent a minimum in the gas phase. The C−C bonds of the pyridine ring are somewhat too long calculated, but apart from that the selected DFT method (B3LYP/6-311++G(d,p)) is proved to be suitable for those investigations.

In the *E*-configured anion (Scheme 6) the (pyridin-4-yl)-methyl moiety and the Cα−Nim bond are located in the same plane from which the naphthyl residue is turned out about 26.2°. The C4−Cα (1.428 Å) and the Cα−Nim (1.331 Å) bond are shortened whereas the Nim−C7 (1.325 Å) bond is elongated in comparison to the neutral species. The pyridine ring is also affected regarding the bond lengths: C2−C3/C5−C6 are somewhat shortened and the remaining bonds are slightly longer (Table 4). The similar bond lengths of Cα−Nim and Nim−C7 remember a 2-aza-allyl anion (mesomeric form **B**, Scheme 5), but the results of the NBO analysis (Table 5) reveal a slight positive charge on C7 (+0.12). The high negative charge on N1 (−0.55) and the carbon atoms C3/5 as well as the extended planar system (pyridine, Cα, Nim, C7) indicate the main contribution of the 4*H*-pyridin-1-ide (form **A**, Scheme 5) on the resonance hybrid.

One possible explanation for the observed attack of the electrophiles at the Cα position (vide infra) is the regeneration of the aromatic system (regain of resonance energy) in the pyridine ring.

The comparison of the experimentally obtained and the calculated ^{13}C NMR signals of ***Z*/*E*-3c** and the *E*-anion **3c(−)** exhibits a little overestimation of the chemical shifts about 4−10 ppm by the theoretical values, but the direction of the changes caused by the negative charge are well reproduced (vide supra).

Table 6. Comparison of the experimental and calculated ^{13}C NMR shifts for selected carbon atoms of ***Z*-3c**, ***E*-3c** and the *E*-anion **3c(−)**, B3LYP/6-311++G(d,p) level of theory (GIAO-DFT calculations[22])

C-atom	Exp. δ (ppm)			Calcd. δ (ppm)		
	***Z*-3c**	***E*-3c**	***E*-3c(−)**	***Z*-3c**	***E*-3c**	***E*-3c(−)**
C2	149.7	149.9	144.8	158.0	158.5	155.0
C3	122.9	123.0	109.8	127.7	128.6	118.6
C4	149.1	149.2	146.6	157.7	157.3	156.4
C5	122.9	123.0	112.4	126.3	126.8	121.0
C6	149.7	149.9	144.7	156.6	156.5	154.9
Cα	55.2	54.9	106.0	60.8	58.9	115.7
C7	171.6	170.8	126.7	179.6	178.7	123.6
C8	29.8	21.1	15.7	33.8	22.2	15.8

Different Lithium Coordination to the 4-(Iminomethyl)pyridine Anion System − A Model Study: Additionally to the experimentally gained results we investigate the monomer coordination modes of the lithium cation to the 4-[(methyleneamino)methyl]pyridine anion with DFT methods. The selected model system derives from 4-(aminomethyl)pyridine (**1**) and formaldehyde (Figure 5, **5**: free anion; **6a**−**d**: lithium species). Those theoretical investigations can be considered as extension to the 4-(picolyl)lithium system formerly examined in our work group.[23]

As depicted in Figure 5, four different coordination modes **6a**−**d** of the lithium cation to the formaldimine anion **5** are conceivable following experimental data[23,24] and theoretical studies,[23,25] whereat π coordination (**6a**−**c**)

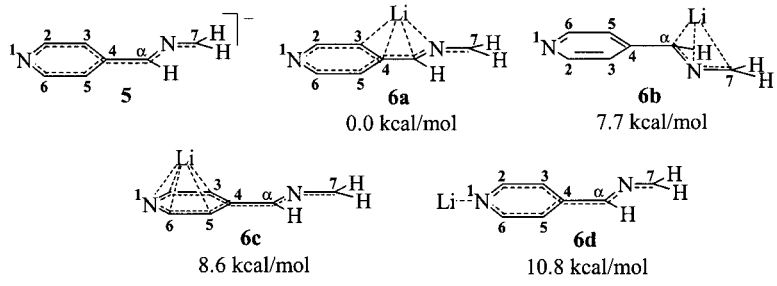

Figure 5. The formaldimine anion **5** and its different coordination modes **6a**−**d** to the lithium counterion

is favored to the Nσ lithiation (**6d**).[26,27] The most stable monomer is structure **6a**, in which the lithium ion is η^4-coordinated to the atoms C3, C4, Cα, and Nim in a sickle-shaped fashion with distinct distortion towards the Nim atom (cf. Table 8 for Li−C/N distances, in Å). This coordination mode was also found in MNDO calculations of Würthwein et al. for lithium 1-phenyl-2-aza-1,3-pentadienyl compounds, in which the lithium is bound to *ortho*-C (Ph ring), *ipso*-C (Ph ring), C1, and N2.[27a] In **6b**, the lithium ion is symmetrically coordinated in an η^3 mode to the atoms Cα, Nim, and C7 in a 2-aza-allyl analogous manner. The Li−C distances are slightly shorter, and the Li−N distance is slightly longer than in **6a**.

The lithium monomer **6c** represents a "borderline" case between η^5 and η^6 coordination because the Li−C4 distance can or cannot be regarded as a binding contact. The Li−C2/6 distances are shorter than the Li−C distances in **6a** and **6b**, but the Li−C3/5 distances in **6c** are clearly longer. The Li−N1 distance is slightly longer than in **6a** and **6b**. In contrary to the lithium coordination observed in the structure motif of **[4e(THF)$_2$]$_2$** (Figure 4), the related monomer model **6d** is the least stable species in this series. This can be attributed to the coordinative unsaturation of the η^1 (Nσ) bound lithium cation. The Li−N1 distance is the shortest one in this series of monomers. The Li−C2/6 distances are too long for binding interactions, but the lithium ion shows a slight shift towards C2 (Table 8). In the solid state (X-ray crystallography),[23] the lithium cation is exclusively coordinated to the N1.

As found in previous investigations of lithium 4-alkylidene-4*H*-pyridin-1-ides in solution (HOESY NMR) stabilization of that mode is achieved by aggregation to dimers (cf. **[4e(THF)$_2$]$_2$**, Figure 4) and additional coordination of solvent molecules (e.g. THF in **[4e(THF)$_2$]$_2$**) or co-ligands (e.g. TMEDA) to obtain a saturation of the metal coordination sphere, which obviously overcompensates the energetically favored π coordination in the monomers.[26b] Collum et al. had shown by NMR investigations that lithio imines and lithio amides form dimers in solution.[28]

Comparing the binding relations of **5** and **6a**−**d** with the experimental bond lengths of the methyleneamino-pyridine moiety in ***Z*-3c** (Table 4) an elongation of the C3−C4/C4−C5 bonds in the anionic systems is discernible, which is greatest for **6c** followed by **6d**. The C4−Cα and Cα−Nim bonds are clearly shortened and therefore have a distinct double bond character, which is greatest for the C4−Cα bond in **6c**,**d** and for the Cα−Nim bond in **6b** and the anions ***E*-3c(−)** (Table 4) and **5**.

The Nim−C7 bond is only slightly lengthened except for **6b** where it is stretched to a similar length of the Cα−Nim bond (an almost symmetrical 2-aza-allyl anion). In **6a**, the C2−C3 bond is strongly stretched in comparison with the naked anion **5** due to the lithium coordination while the C3−C4 and C4−Cα bonds are only slightly affected. The

Table 7. Absolute and relative energies for the calculated structures of the anion **5** and the four lithium isomers **6a**−**d**

Structure	abs. E[a] [a.u.]	ZPE [a.u.]	ZPE-corr. E [a.u.]	rel. E ΔE [kcal·mol^{-1}]	NIMAG[b]
5	−380.566295	0.122602	−380.443693	−	[0]
6a	−388.080721	0.126578	−387.954143	0.0	[0]
6b	−388.067755	0.125956	−387.941799	7.7	[0]
6c	−388.067050	0.126564	−387.940486	8.6	[0]
6d	−388.062981	0.126026	−387.936955	10.8	[0]

[a] B3LYP/6-311++G(d,p) optimizations. [b] *N*umber of *imag*inary frequencies.

Table 8. Calculated bond lengths and distances to lithium (in Å) of the anion **5** and the lithium species **6a**−**d**

Bond	**5**	**6a**	**6b**	**6c**	**6d**
N1−C2	1.353	1.330	1.342	1.371	1.381
N1−C6	1.349	1.356	1.339	1.368	1.377
C2−C3	1.380	1.397	1.387	1.378	1.359
C3−C4	1.432	1.438	1.410	1.457	1.447
C4−C5	1.431	1.430	1.409	1.454	1.445
C5−C6	1.381	1.375	1.389	1.380	1.361
C4−Cα	1.408	1.418	1.453	1.377	1.379
Cα−Nim	1.348	1.373	1.336	1.373	1.370
Nim-C7	1.299	1.296	1.329	1.283	1.284
		Li−Nim 1.910	Li−Cα 2.147	Li−N1 2.055	Li−N1 1.805
		Li−Cα 2.161	Li−Nim 1.919	Li−C2 2.121	
		Li−C4 2.195	Li−C7 2.151	Li−C3 2.276	Li−C2 2.786
		Li−C3 2.171		Li−C4 2.423	Li−C6 2.822
				Li−C5 2.288	
				Li−C6 2.131	

lithium η^5/η^6 coordination in **6c** causes a strong elongation of the N1−C2/N1−C6 bonds in comparison with the neutral ***Z*-3c** and the naked anion **5**, while the C2−C3/C5−C6 bonds are barely influenced. The isomer **6d** show an lengthening of N1−C2/N1−C6 bonds as well, but is accompanied with a shortening of the C2−C3/C5−C6 and C4−Cα bonds.

The NBO analysis of the anion **5** reveals five centers with increased negative charge density: N1, C3/C5, Cα, Nim, and C7. The interaction with the lithium cation changes the charge distribution as expected in direction to the coordinating centers. In **6a**, C3, C4, Cα, and Nim bear a higher negative charge, C7 a smaller one than in **5**. The lithium 2-aza-allyl isomer **6b** shows a high negative charge on C7 and Cα; the charge on the imine nitrogen is a little bit smaller than in **6a**. Coordination of the metal ion above the pyridine ring plane in **6c** causes the accumulation of negative charge into the ring, which results in the negativation of C2/C6. The Nσ interaction of the lithium ion in **6d** entails a high concentration of negative charge onto the pyridine nitrogen N1.

In contrast to **5**, the highly substituted anion ***E*-3c(−)** (Table 5) contains only four centers of higher negative charge density: N1, C3/5, Cα, and Nim. The carbon C7 is positively charged (about the same amount like Cα), which should be traced back to the bulky naphthalene residue. This result is more consistent with the experimental observations of favoring the Cα attack.

Table 9. Calculated charge distribution of the anion **5** and the lithium species **6a**−**d** as result of an NBO analysis (B3LYP/6-311++G(d,p) level of theory, NBO version 3.0[21]); charges of the hydrogen atoms are omitted

Atom	**5**	**6a**	**6b**	**6c**	**6d**
N1	−0.59	−0.52	−0.49	−0.66	−0.88
C2	0.02	0.09	0.05	−0.05	0.01
C3	−0.29	−0.46	−0.26	−0.34	−0.26
C4	−0.05	−0.11	−0.05	−0.11	−0.06
C5	−0.30	−0.27	−0.26	−0.34	−0.26
C6	0.02	0.05	0.05	−0.05	0.02
Cα	−0.16	−0.23	−0.26	−0.12	−0.11
Nim	−0.45	−0.60	−0.51	−0.46	−0.45
C7	−0.28	−0.16	−0.45	−0.11	−0.13
Li	−	0.93	0.92	0.94	0.95

Reactions with Heterocumulenes − an Outlook

Two trendsetting examples are described here to give a first expression on the chemical behavior of the lithium 4*H*-pyridin-1-ides **4** towards heterocumulenes X=C=Y: the reaction of **4e** with carbon dioxide[29] and phenyl isocyanate (**8**), respectively (Scheme 7 and 8).

Bubbling dry carbon dioxide gas through a clear, deep red THF solution of **4e** at room temp. causes an instantaneous change of color to bright yellow, a slight warming of the solution (5−10 °C) and the formation of a voluminous, fluffy precipitate. The reaction is completed after less than 5 min.

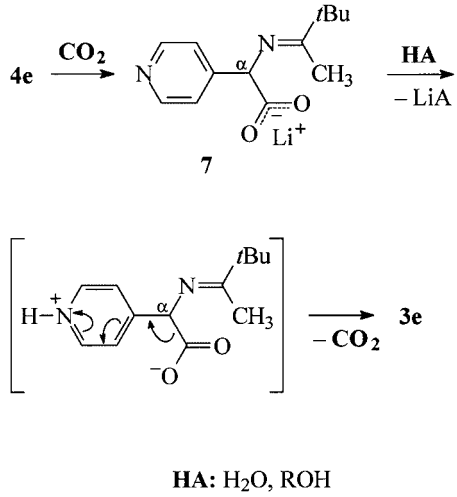

Scheme 7. Formation and decay of the carboxylate **7** under mild protic conditions

As 2D NMR measurements exhibit the attack of CO_2 occurs on the Cα atom, which results in formation of the lithium 2-[(dialkylmethylene)amino]-2-(pyridin-4-yl)acetate **7**. In the HMBC spectrum ($^1H,^{13}C$ correlation) the crosspeaks between Hα and C7 (imine carbon) and C13 (carboxyl carbon), respectively, unambiguously pinpoint the carboxyl group to the α position. If CO_2 would be bound on C7 a crosspeak between the methyl protons and the carboxyl carbon have to appear, but such a signal was not observed. The carboxylate experienced a fast loss of carbon dioxide in protic solvents (like water or alcohols) under recovery of the starting material imine **3e**. Presumably, the proton is primarily attached to the pyridine nitrogen as in an amino acid zwitterion, which facilitates the escape of CO_2 via formation of a neutral 4-alkylidene-1,4-dihydropyridine. Spontaneous decarboxylation is also described for other free pyridin-4/2-yl acetic acids.[30] Thus, the 4*H*-pyridin-1-ide anion in **4e** is able to act as carbon dioxide reservoir by fixation and release of CO_2 following the vitamin B_6 similar way (Scheme 2, b) under mild conditions. Attempts to isolate the corresponding hydrochloride of the acid failed due to the large pace of the decarboxylation and the instability of the imine functionality against an acidic

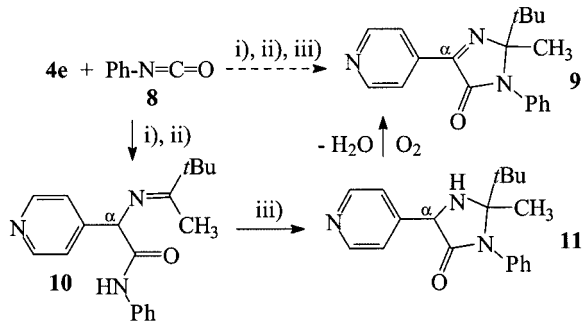

Scheme 8. Reaction sequence leading to the (pyridin-4-yl)-5(2*H*)-imidazolone **9**. i) THF, −30 °C to room temp.; ii) $H_2O/CHCl_3$; iii) CH_3OH/O_2 (air), Δ*T*

medium. Derivatization reactions for carboxyl anions to get a more stable carboxyl system like an ester or an amide are rare. But it turned out that the ethyl ester prepared from **4e** and diethyl carbonate is unstable against protic solvents, too (formation of CO_2 and ethanol).

The addition of phenyl isocyanate (**8**) to a solution of **4e** followed by hydrolysis and treating the crude product with hot methanol resulted in the 4-(pyridin-4-yl)-5(2*H*)-imidazolone **9** (Scheme 8). Based on NMR spectroscopic data the crude foamy product obtained after hydrolysis consists mainly of the carboxamide **10** resulting from the attack on the Cα atom of **4e**. The percentage of **10** in the foam amounts to 70−95% in dependence of the working-up rate. The attempt to obtain **10** in pure substance by crystallization or column chromatography failed due to the fast cyclization-oxidation or the decomposition of the imino function. Heating **10** in methanol for several minutes under vigorous stirring causes ring closure and oxidation of the CαH−NH bond of the built imidazolidone derivative **11** to **9**. Compound **11** was only observable in NMR spectra (cf. Exp. Sect.) during the oxidation process. The carboxamide **10** and the imidazolidone **11** differ clearly from each other in the chemical shift of the Hα and the NH signal in the ^{1}H NMR spectrum (**10**: Hα δ = 5.00, NH 9.86 ppm; **11**: Hα δ = 4.64, NH 9.46 ppm). The structural determination of **9** was carried out with two-dimensional NMR spectroscopy. The result of the reaction sequence can be grasped in the widest sense as 1,3-dipolar cycloaddition (**11**) followed by an oxidation (**9**). The formation of an extended conjugated π-system between aromatic pyridine ring and C=O double bond is considered as driving force for the oxidation.

The 1,3-dipolar cycloaddition of azomethine ylides, derived from the thermal ring opening of aziridines, or other nitrogen ylides with iso(thio)cyanates resembles on the above presented reaction, but a following oxidation is often not possible due to the substituent on the aziridine N atom (not a proton).[31]

Conclusion

A new class of azomethines is easily synthesized by condensation of 4-(aminomethyl)pyridine with various ketones. The unsymmetrically substituted imines can appear in *E*/*Z* isomers but only in one case (**3c**) both isomers could be observed at NMR spectroscopy. DFT calculations give insights on mechanistical details of the *E*/*Z* isomerization of the imines; according to them it takes place via an inversion. The α-methylene group shows a remarkable CH acidity and can be deprotonated almost completely by *n*-butyllithium. Comparison of the NMR spectra of the azomethine starting materials **3** and the corresponding anions **4** allows a conclusion on the delocalization of the negative charge into the pyridine ring and the C=N double bond. This is supported by DFT calculations on a model system derived from 4-(aminomethyl)pyridine and formaldehyde. According the DFT results, the sickle-shaped η^4 coordination mode of lithium in **6a** is the most stable found monomer species in the gas phase. The *E* configuration of two lithium compounds (**4c**,**e**) could be proved by a NOESY experiment and a structure motif, respectively. On the contrary to the calculated charge distribution the attack of different heterocumulenes preferentially occurs on the α-carbon. The carboxylate **7** obtained as product of treating **4e** with CO_2 undergoes a fast decarboxylation under mild protic conditions and, thus, can serve as a CO_2 storage. The primarily formed carboxamide **10** by reaction of **4e** with phenyl isocyanate and following hydrolysis cyclizes to the imidazolidinone **11** which is easily oxidized on the CαH−NH bond to the imidazol-4-one **9**.

Experimental Section

General Remarks: Spectra were measured with following technical devices: NMR − Bruker AC 250 and AC 400, respectively, IR-ATR − BIORAD FTS-25, MS − Finnigan MAT SSQ 710 and Finnigan MAT 900 XL TRAP, respectively. Elemental analyses (C, H, N, S) − Leco CHNS-932 and Vario EL III. NMR spectra were recorded at 250 or 400 MHz and 62.5 or 100 MHz, for proton and carbon, respectively. For ^{1}H and ^{13}C, [D$_8$]THF (δ_H = 1.73, 3.58 ppm, δ_C = 25.2, 67.4 ppm) and $CDCl_3$ (δ_H = 7.24, δ_C = 77.0 ppm) were used as solvents with TMS as internal standard. Melting points (uncorrected) were obtained with a Lindstrom copper block apparatus. The ketones **2a**−**e** and 4-(aminomethyl)pyridine (**1**) are commercially available, but ketones **2b**,**c**,**d** were prepared in Friedel−Crafts acylation according to standard procedure. The amine **1** was purified by distillation and used immediately. *n*-Butyllithium (1.6 M solution in hexane fraction) were purchased from Aldrich. The diethylmagnesium solution was prepared after literature procedure.[32] The concentration of magnesium was determined by titration with 0.025 M EDTA solution against Eriochromscharz T. The nomenclature of all new compounds was obtained using the programme ACD/IUPAC Name Free v8.05 with the ACD/I-Lab service. For more information about ACD/IUPAC Name Free v8.05 for Windows, please contact ACD (www.acdlabs.com).

General Procedure for the Synthesis of 3a−e: A solution of ketone **2** (0.1 mol), amine **1** (0.1 mol) and *p*-toluenesulfonic acid (75−100 mg) in toluene (125 mL) was refluxed in a Dean−Stark apparatus until almost all reaction water (0.1 mol) has separated (5−14 h). After cooling to room temp. the reaction solution is washed with diluted Na_2CO_3 solution (1 × 75 mL), brine (3 × 75 mL) and dried with Na_2SO_4. Further purification was carried out as described at the corresponding imine **3**.

***N*-(Diphenylmethylene)-(1-pyridin-4-yl)methanamine (3a):** Reflux: 14 h. After complete removal of toluene in vacuo the resulting yellow oil was crystallized with diethyl ether (30 mL), maybe under cooling. The imine precipitated as pale yellow powder. From the filtrate pale yellow crystal were obtained after cooling to + 4 °C. Yield: 16.1 g (59%), m.p. 236−238 °C (decomposition). ^{1}H NMR (250 MHz, $CDCl_3$, room temp.): δ = 4.56 (s, 2 H), 7.14−7.18 (m, 2 H), 7.28 (dd, ^3J = 4.43, ^4J = 1.75 Hz, 2 H), 7.33−7.38 (m, 3 H), 7.43−7.47 (m, 3 H), 7.66−7.70 (m, 2 H), 8.52 (dd, ^3J = 4.43, ^4J = 1.75 Hz, 2 H) ppm. ^{13}C NMR (62.5 MHz, $CDCl_3$, room temp.): δ = 56.1, 122.7, 127.5, 128.2, 128.5, 128.7, 128.8, 130.4, 136.3, 139.3, 149.7, 170.2 ppm. IR (ATR): $\tilde{\nu}$ = 3025 (=C−H), 1622 (C=N), 1596 (aryl), 1444 (CH_2) cm^{-1}. MS (ESI): *m*/*z* (%) = 273 (100)

[M + H]. $C_{19}H_{16}N_2$ (272.34): calcd. C 83.79, H 5.92, N 10.29; found C 83.73, H 5.91, N 10.34.

***N*-[1-(4-Phenylphenyl)ethylidene]-(1-pyridin-4-yl)methanamine (3b):** Reflux: 10 h. The solution was concentrated to one third of the original volume and cooled to +4 °C. The yellow precipitate was filtered off and washed with cold diethyl ether. From the filtrate another fraction could be collected. The imine is sufficiently pure for further reactions, but additional purification is possible by extraction with *n*-hexane. Yield: 15.2 g (53%), m.p. 100 °C (decomposition). ^{1}H NMR (250 MHz, $CDCl_3$, room temp.): δ = 2.35 (t, ^5J = 0.78 Hz, 3 H), 4.70 (s, 2 H), 7.34−7.47 (m, 5 H), 7.61 (dd, ^3J = 8.35, ^4J = 1.43 Hz, 2 H), 7.63 (dd, ^3J = 8.70, ^4J = 2.08 Hz, 2 H), 7.95 (dd, ^3J = 8.53, ^4J = 1.90 Hz, 2 H), 8.57 (dd, ^3J = 4.43, ^4J = 1.58 Hz, 2 H) ppm. ^{13}C NMR (62.5 MHz, $CDCl_3$, room temp.): δ = 16.0, 54.4, 122.8, 127.0, 127.1, 127.2, 127.7, 139.4, 140.4, 142.7, 149.7, 149.8, 166.6 ppm. IR (ATR): $\tilde{\nu}$ = 3029 (=C−H), 1679 (C=N), 1600 (aryl), 1412 (CH_2) cm^{-1}. MS (Micro-ESI): *m*/*z* (%) = 287 (100) [M + H]. $C_{20}H_{18}N_2$ (286.37): calcd. C 83.88, H 6.34, N 9.78; found C 83.50, H 6.24, N 9.74.

***N*-[1-(1-Naphthyl)ethylidene]-(1-pyridin-4-yl)methanamine (3c):** Reflux: 4−5 h. Working up like **3b**: beige needles, which can be recrystallized from *n*-hexane. Yield: 15.6 g (60%), m.p. 87−90 °C. ^{1}H NMR (400 MHz, $CDCl_3$, room temp.), ***Z*-3c:** δ = 2.49 (t, ^5J = 1.28 Hz, 3 H), 4.19 (m_{AB}, 2 H), 7.13 (dd, ^3J = 4.40, ^4J = 1.44 Hz, 2 H), 7.18 (dd, ^3J = 6.96, ^4J = 1.00 Hz, 1 H), 7.46−7.54 (m, 3 H), 7.61 (dd, ^3J = 7.40, ^4J = 1.08 Hz, 1 H), 7.85 (d, ^3J = 8.24 Hz, 1 H), 7.90 (dd, ^3J = 7.16, ^4J = 1.76 Hz, 1 H), 8.47 (dd, ^3J = 4.52, ^4J = 1.52 Hz, 2 H) ppm. ***E*-3c:** 2.44 (t, ^5J = 0.7−0.8 Hz, 3 H), 4.79 (s, 2 H), 7.41 (dd, ^3J = 4.48, ^4J = 1.52 Hz, 2 H), 8.04 (d, ^3J = 9.76 Hz, 1 H), 8.56 (dd, ^3J = 4.40, ^4J = 1.52 Hz, 2 H) ppm. ^{13}C NMR (100 MHz, $CDCl_3$, room temp.), ***Z*-3c:** δ = 29.8, 55.2, 122.89, 122.94, 124.4, 125.5, 126.6, 127.1, 128.5, 128.6, 128.8, 133.4, 137.3, 149.1, 149.7, 171.6 ppm. ***E*-3c:** 21.1, 54.9, 123.0, 124.4, 125.2, 126.0, 125.2, 125.0, 129.1, 130.0, 133.8, 140.7, 149.2, 149.9, 170.8 ppm. IR (ATR): $\tilde{\nu}$ = 3053 (=C−H), 1643 (C=N), 1600 (aryl), 1414 (CH_2) cm^{-1}. MS (EI): *m*/*z* (%) = 259 (100) [M − H$^+$]. $C_{18}H_{16}N_2$ (260.33): calcd. C 83.03, H 6.21, N 10.76; found C 83.22, H 6.31, N 10.73.

***N*-[1-(4-Methoxyphenyl)ethylidene]-(1-pyridin-4-yl)methanamine (3d):** Reflux: 3−4 h. Toluene was completely removed and the dark yellow solid was extracted with *n*-hexane. After cooling to +4 °C a white precipitate could be isolated. The imine must be stored under argon as it decomposes quickly due to reaction with air moisture. Yield: 14.4 g (60%), m.p. 78−80 °C (decomposition). ^{1}H NMR (250 MHz, $CDCl_3$, room temp.): δ = 2.32 (s, 3 H), 3.86 (s, 3 H), 4.69 (s, 2 H), 6.94 (dd, ^3J = 6.79, ^4J = 2.15 Hz, 2 H), 7.42 (dd, ^3J = 4.45, ^4J = 1.54 Hz, 2 H), 7.88 (d, ^3J = 6.82, ^4J = 2.11 Hz, 2 H), 8.59 (dd, ^3J = 4.44, ^4J = 1.59 Hz, 2 H) ppm. ^{13}C NMR (62.5 MHz, $CDCl_3$, room temp.): δ = 15.7, 54.2, 55.3, 113.7, 122.8, 128.2, 130.6, 133.3, 149.9, 150.0, 161.1, 166.2 ppm. IR (ATR): $\tilde{\nu}$ = 3004 (=C−H), 1675, 1629, 1597 (aryl), 1411 (CH_2) ppm. MS (ESI): *m*/*z* (%) = 241 (100) [M + H]$^+$. $C_{15}H_{16}N_2O$ (240.30): calcd. C 74.97, H 6.71, N 11.66, O 6.67; found C 74.71, H 6.70, N 11.48.

1-(Pyridin-4-yl)-*N*-(1,2,2-trimethylpropylidene)methanamine (3e): Reflux: 5 h. After completely evaporating the solvent the yellow oil was purified by distillation. The white liquid crystallized at rubbing with a glass stick. The imine must be also stored under argon. Yield: 14.1 g (74%), b.p. 108−110 °C (0.2 mbar), m.p. 38−42 °C. ^{1}H NMR (250 MHz, $CDCl_3$, room temp.): δ = 1.17 (s, 9 H), 1.86 (s, 3 H), 4.43 (s, 2 H), 7.31 (d, ^3J = 5.00 Hz, 2 H), 8.53 (d, ^3J = 5.00 Hz, 2 H) ppm. ^{13}C NMR (62.5 MHz, $CDCl_3$, room temp.): δ = 13.8, 27.7, 40.9, 53.2, 122.5, 149.6, 150.3, 177.6 ppm. IR (ATR): $\tilde{\nu}$ = 3028 (=C−H), 2967 (CH_2, CH_3), 1652 (C=N), 1600, 1557, 1472 (aryl), 1410 (CH_2, CH_3) cm^{-1}. MS (EI): *m*/*z* (%) = 191 (100) [M + H]$^+$. $C_{12}H_{18}N_2$ (190.28): calcd. C 75.73, H 9.55, N 14.72; found C 75.67, H 9.51, N 15.06.

General Procedure for the Synthesis of 4a−e: The compounds **4a−e** were directly prepared for NMR in deuterated [D$_8$]THF without prior isolation. The synthesis is carried out under argon. A yield would not given since a very small inaccuracy can already lead to an incomplete deprotonation. In a small Schlenk tube 0.3 mL (0.48 mmol) *n*-butyllithium (1.6 M solution in hexane) is filled in and the solvent is removed completely by distillation (cold). The oily residue is dried in vacuo for 1 1/2 h and then dissolved in 0.3−0.5 mL [D$_8$]THF. To a −70 °C cold solution of 0.48 mmol imine **3** in 0.8−1.0 mL [D$_8$]THF the freshly prepared *n*-butyllithium solution is added dropwise about a period of 10 minutes. Subsequently the cooling is removed. The reaction mixture is stirred overnight and then 0.5 mL are filled into a NMR tube.

Lithium 4-{[(Diphenylmethylene)amino]methylene}-4*H*-pyridin-1-ide (4a): ^{1}H NMR (250 MHz, [D$_8$]THF, room temp.): δ = 5.73 (dd, ^3J = 6.13, ^4J = 1.23 Hz, 2 H), 6.04, (s, 1 H), 6.65 (t, ^3J = 7.16 Hz, 1 H), 6.93 (t, ^3J = 7.36 Hz, 2 H), 7.01 (d, ^3J = 6.12 Hz, 1 H), 7.11−7.17 (m, 5 H), 7.31 (t, ^3J = 8.14 Hz, 2 H), 7.42 (dd, ^3J = 8.53, ^4J = 1.15 Hz, 2 H) ppm. ^{13}C NMR (62.5 MHz, [D$_8$]THF, room temp.): δ = 106.8, 111.7, 113.5, 121.5, 124.2, 125.9, 127.7, 128.8, 130.4, 131.6, 141.5, 145.0, 145.3, 145.7, 148.1 ppm.

Lithium 4-({[(1*E*)-1-(4-Phenylphenyl)ethylidene]amino}methylene)-4*H*-pyridin-1-ide (4b): ^{1}H NMR (250 MHz, [D$_8$]THF, room temp.): δ = 2.02 (s, 3 H), 6.02 (dd, ^3J = 6.20, ^4J = 2.11 Hz, 1 H), 6.19 (s, 1 H), 7.09−7.18 (m, 4 H), 7.33 (t, ^3J = 7.88 Hz, 2 H), 7.38 (d, ^3J = 8.87 Hz, 2 H), 7.59 (dd, ^3J = 8.50, ^4J = 1.32 Hz, 2 H), 7.74 (d, ^3J = 8.67 Hz, 2 H) ppm. ^{13}C NMR (62.5 MHz, [D$_8$]THF, room temp.): δ = 11.1, 105.9, 110.6, 112.9, 122.7, 123.6, 125.2, 125.3, 125.4, 128.2, 132.2, 141.8, 143.7, 144.5, 144.9, 146.6 ppm.

Lithium 4-({[(1*E*)-1-(1-Naphthyl)ethylidene]amino}methylene)-4*H*-pyridin-1-ide (4c): ^{1}H NMR (400 MHz, [D$_8$]THF, 0 °C): δ = 2.22 (s, 3 H), 5.99 (dd, ^3J = 6.21, ^4J = 2.04 Hz, 1 H), 6.21 (s, 1 H), 6.95 (dd, ^3J = 6.31, ^4J = 1.91 Hz, 1 H), 7.05 (d, ^3J = 6.20 Hz, 1 H), 7.07 (d, ^3J = 6.33 Hz, 1 H), 7.18−7.25 (m, 5 H), 7.58 (d, ^3J = 9.55 Hz, 1 H), 9.65 (d, ^3J = 9.87 Hz, 1 H) ppm. ^{13}C NMR (100 MHz, [D$_8$]THF, 0 °C): δ = 15.7, 106.0, 109.8, 112.4, 121.3, 121.5, 123.2, 124.0, 124.8, 126.9, 130.5, 131.7, 135.2, 142.2, 144.7, 144.8, 146.6 ppm.

Lithium 4-({[(1*E*)-1-(4-Methoxyphenyl)ethylidene]amino}methylene)-4*H*-pyridin-1-ide (4d): ^{1}H NMR (250 MHz, [D$_8$]THF, room temp.): δ = 1.93 (s, 3 H), 3.68 (s, 3 H), 5.79 (dd, ^3J = 6.33, ^4J = 2.23 Hz, 1 H), 5.96 (s, 1 H), 6.64 (dd, ^3J = 6.95, ^4J = 2.23 Hz, 2 H), 6.81 (dd, ^3J = 6.33, ^4J = 2.05 Hz, 1 H), 6.89 (d, ^3J = 6.15 Hz, 1 H), 6.96 (d, ^3J = 6.33 Hz, 1 H), 7.59 (dd, ^3J = 6.95, ^4J = 2.23 Hz, 2 H) ppm. ^{13}C NMR (62.5 MHz, [D$_8$]THF, room temp.): δ = 11.2, 54.2, 103.7, 109.4, 111.6, 112.6, 123.6, 125.2, 138.1, 144.0, 144.2, 145.1, 155.7 ppm.

Lithium 4-({[(1*E*)-1,2,2-Trimethylpropylidene]amino}methylene)-4*H*-pyridin-1-ide (4e): ^{1}H NMR (250 MHz, [D$_8$]THF, room temp.): δ = 1.09 (s, 9 H), 1.66 (s, 3 H), 5.56 (s, 1 H), 5.51 (dd, ^3J = 6.42, ^4J = 2.19 Hz, 1 H), 6.41 (dd, ^3J = 6.54, ^4J = 2.28 Hz, 1 H), 6.67 (d, ^3J = 6.41 Hz, 1 H), 6.73 (d, ^3J = 6.51 Hz, 1 H) ppm. ^{13}C NMR (62.5 MHz, [D$_8$]THF, room temp.): δ = 10.8, 28.3, 38.8, 99.4, 107.4, 109.1, 138.4, 142.7, 143.2, 143.3 ppm.

Potassium 4-({[(1*E*)-1-(1-Naphthyl)ethylidene]amino}methylene)-4*H*-pyridin-1-ide [K3c(−)]: The preparation is carried out with standard Schlenk technique. To a solution of $KN(SiMe_3)_2$ (0.751 g, 3.76 mmol) in diethyl ether (30 mL) **3c** (0.979 g, 3.76 mmol) is added in small portions at 0 °C, whereat the color changes immediately to dark blue violet. After 3 h stirring at room temp. an half oily, half crystalline precipitate is formed, which becomes solid at standing overnight. The solution is decanted and the dark blue violet residue is washed twice with 10 mL diethyl ether and then dried in vacuo. Yield: 1.10 g (83%) (0.75 molecules of diethyl ether included). ^{1}H NMR ([D$_8$]THF, 250 MHz): δ = 2.22 (s, 3 H), 6.12 (d, ^3J = 5.63 Hz, 1 H), 6.18 (s, 1 H), 6.88 (dd, ^3J = 5.71, ^4J = 153 Hz, 1 H), 7.17−7.39 (m, 7 H), 7.60 (d, ^3J = 6.83 Hz, 1 H), 9.46 (d, ^3J = 9.98 Hz, 1 H) ppm. ^{13}C NMR ([D$_8$]THF, 62.5 MHz): δ = 14.3, 102.7, 106.9, 111.4, 118.9, 119.0, 121.5, 122.3, 123.2, 125.3, 128.1, 129.4, 133.7, 140.0, 145.1, 145.4, 145.6, 147.5 ppm.

Magnesium Bis[4-({[(1*E*)-1-(1-naphthyl)ethylidene]amino}methylene)-4*H*-pyridin-1-ide] {Mg[3c(−)]$_2$}: The preparation was carried out with standard Schlenk technique. To a solution of 3c (1.102 g, 4.23 mmol) in THF (20 mL) a $MgEt_2$ solution (4.0 mL, c = 0.53 mol/L in THF)[32] is added at −20 °C over a period of 40 min, whereat the color changes from beige to orange-brown with a violet touch. The solution is warmed up to room temp. and stirred at room temp. for 3 h. Over night the solution takes on an intensive blue-violet color and precipitate of small red crystals is formed, which is isolated and dried in vacuo. Yield: 1.53 g (52%) (2.1 molecules of THF included). ^{1}H NMR ([D$_6$]DMSO, 250 MHz): δ = 2.15 (s, 3 H), 6.03 (d, ^3J = 4.35 Hz, 1 H), 6.11 (s, 1 H), 6.79 (d, ^3J = 4.51 Hz, 1 H), 7.19−7.35 (m, 7 H), 7.70 (dd, ^3J = 7.45, ^4J = 3.46 Hz, 1 H), 9.50 (dd, ^3J = 5.85, ^4J = 3.85 Hz, 1 H) ppm. ^{13}C NMR ([D$_6$]DMSO, 62.5 MHz): δ = 16.5, 105.5, 108.9, 112.2, 121.1, 121.2, 123.8, 124.6, 125.3, 127.4, 129.4, 130.6, 134.7, 141.1, 146.0, 149.3, 149.4 ppm.

Lithium Pyridin-4-yl[(1,2,2-trimethylpropylidene)amino]acetate (7): To a −78 °C cold solution of **3e** (0.913 g, 4.8 mmol) in THF (20 mL), *n*BuLi (3.0 mL, 4.8 mmol, 1.6 M solution in hexane) are added dropwise over a period of 30−40 min. The resulting deep red solution is allowed to come to room temp. and stirred overnight. Dry carbon dioxide gas is bubbled through the solution at room temp. whereat the color changes instantaneously to bright yellow, the temperature raises slightly (5−10 °C) and a voluminous precipitate is formed. The filtered product is carefully dried in vacuo (2 d). Because of varying amounts of THF in the product the exact yield cannot be given. Yield: 1.12 g (73%) (1.1 molecules of THF included). ^{1}H NMR ([D$_6$]DMSO, room temp.): δ = 1.09 (s, 9 H), 1.73 (s, 3 H), 4.82 (s, 1 H), 7.47 (d, ^3J = 6.15 Hz, 2 H), 8.37 (d, ^3J = 5.83, ^4J = 1.40 Hz, 2 H) ppm. ^{13}C NMR ([D$_6$]DMSO, room temp.): δ = 14.2, 27.5, 39.7, 69.9, 122.9, 148.5, 152.1, 172.3, 176.5 ppm. IR (ATR): $\tilde{\nu}$ = 2963, 2871, 1643, 1604, 1364, 1304 cm^{-1}. MS (ESI negative): *m*/*z* (%) = 473 (39) $[Li(C_{13}H_{17}N_2O_2)_2]^-$, 713 (63) $[Li_2(C_{13}H_{17}N_2O_2)_3]^-$.

2-*tert*-Butyl-2-methyl-3-phenyl-5-(pyridin-4-yl)-2,3-dihydro-4*H*-imidazol-4-one (9): To a −78 °C cold solution of **3e** (0.913 g, 4.8 mmol) in 20 mL THF, *n*BuLi (3.0 mL, 4.8 mmol, 1.6 M solution in hexane) were added dropwise over a period of 30−40 min. The resulting deep red solution was allowed to come to room temp. and stirred overnight. After addition of 0.525 mL (4.8 mmol) phenyl isocyanate (**8**) to the solution at −30 °C the cooling was removed. A very voluminous orange precipitate formed after 15 min, which stands for 6 h at room temp. The following workup was carried out under not-inert conditions. The solvent was almost evaporated to dryness, the residue hydrolyzed with 30 mL water, the water phase extracted with $CHCl_3$ (3 × 30 mL), the organic layer was washed with brine (1 × 50 mL), and dried with Na_2SO_4. The chloroform was completely removed resulting in a yellow foam, which consists mainly of the carboxamide **10**. The attempt to obtain **10** in purified form by crystallization or column chromatography failed due to the fast cyclization-oxidation or the decomposition of the imino function.

***N*-Phenyl-2-(pyridin-4-yl)-2-[(1,2,2-trimethylpropylidene)amino]-acetamide (10):** (As crude product, ca 80%): ^{1}H NMR ($CDCl_3$, 250 MHz): δ = 1.29 (s, 9 H), 1.80 (s, 3 H), 5.00 (s, 1 H), 7.12 (t, ^3J = 7.39 Hz, 1 H), 7.29−7.39 (m, 4 H), 7.58 (d, ^3J = 7.47 Hz, 2 H), 8.57 (dd, ^3J = 4.50, ^4J = 1.62 Hz, 2 H), 9.86 (br. s, 1 H,) ppm. ^{13}C NMR ($CDCl_3$, 62.5 MHz): δ = 15.0, 26.4, 41.3, 66.3, 119.4, 122.0, 129.0, 129.6, 137.5, 147.6, 149.8, 168.8, 181.0 ppm. IR (ATR): $\tilde{\nu}$ = 3278 (NH), 3060, 3034, 2969 (alkyl), 1697 (C=O), 1597, 1546, 1496, 1443, 1369, 1307 cm^{-1}. MS (Micro-ESI): *m*/*z* (%) = 332 (100) $[M + Na]^+$. Exact mass for $C_{19}H_{23}N_3ONa$ calcd. 332.174; found 332.174. The yellow foam was dissolved in 30 mL methanol and the solution heated for 10 min while bubbling air through it. Evaporation of the solvent gives the 4*H*-imidazol-4-one **9**, which is contaminated with 13−15% of the imidazolidin-4-one **11**, in 49% yield.

2-*tert*-Butyl-2-methyl-3-phenyl-5-(pyridin-4-yl)imidazolidin-4-one (11): (Not isolated). ^{1}H NMR ($CDCl_3$, 250 MHz): δ = 1.15 (s, 9 H), 2.16 (s, 3 H), 4.64 (s, 1 H), 7.29−7.41 (m, 7 H), 8.60 (dd, ^3J = 4.49, ^4J = 1.67 Hz, 2 H), 9.46 (br. s, 1 H) ppm. ^{13}C NMR ($CDCl_3$, 62.5 MHz): δ = 24.7, 44.3, 59.4, 77.3, 119.6, 121.9, 124.6, 129.0, 129.6, 149.1, 149.9, 169.6 ppm. The crude product **9** can be purified by column chromatography: Silica gel 60 (0.063−0.2 mm, Fluka), eluent ethyl acetate. **2-*tert*-Butyl-2-methyl-3-phenyl-5-(pyridin-4-yl)-2,3-dihydro-4*H*-imidazol-4-one (9):** Isolated yield: 0.190 g (12.8%), m.p. 106−108 °C. ^{1}H NMR ($CDCl_3$, 250 MHz): δ = 0.94 (s, 9 H), 1.87 (s, 3 H), 7.26−7.51 (m, 5 H), 8.31 (dd, ^3J = 4.54, ^4J = 1.50 Hz, 2 H), 8.77 (d, ^3J = 5.93 Hz, 2 H) ppm. ^{13}C NMR ($CDCl_3$, 62.5 MHz): δ = 21.4, 25.9, 39.9, 93.6, 122.0, 127.5, 128.2, 129.6, 137.4, 137.7, 150.4, 160.0, 162.7 ppm. IR (ATR): $\tilde{\nu}$ = 3067, 3051, 2956, 2875, 1697, 1596, 1499, 1412, 1387, 1368, 1306, 1125 cm^{-1}. MS (Micro-ESI): *m*/*z* (%) = 330 (100) $[M + Na]^+$. $C_{19}H_{21}N_3O$ (307.39): calcd. C 74.24, H 6.89, N 13.67, O 5.20; found C 74.59, H 6.95, N 13.94.

Crystal Structure Determination: The intensity data for the compounds were collected on a Nonius KappaCCD diffractometer, using graphite-monochromated Mo-K_α radiation. Data were corrected for Lorentz and polarization effects, but not for absorption.[33,34] The structures were solved by direct methods (SHELXS[35]) and refined by full-matrix least-squares techniques against F_o^2 (SHELXL-97[36]). The hydrogen atoms for the compound ***Z*-3c** were located by difference Fourier synthesis and refined isotropically. All other hydrogen atoms were included at calculated positions with fixed thermal parameters. The absolute configuration of compound ***Z*-3c** could not be determined. All non-hydrogen atoms were refined anisotropically.[36] XP (SIEMENS Analytical X-ray Instruments, Inc.) was used for structure representations.

Crystal Data for [4e(THF)$_2$]$_2$:[37] $C_{40}H_{66}Li_2N_4O_4$, Mr = 680.85 g·mol^{-1}, colourless prism, size 0.05 × 0.04 × 0.04 mm^3, orthorhombic, space group *Cmca*, a = 13.8551(3), b = 12.4606(2), c = 24.7271(6) Å, V = 4268.96(15) Å^3, T = −90 °C, Z = 4, $\rho_{calcd.}$ = 1.059 g·cm^{-3}, μ(Mo-K_α) = 0.67 cm^{-1}, F(000) = 1488, 13819 reflections in h(−16/17), k(−16/14), l(−29/32), measured in the range 4.40° ≤ Θ ≤ 27.46°, completeness $\Theta_{max.}$ = 99.2%, 2523 indepen-

dent reflections, R_{int} = 0.055, 1604 reflections with $F_o > 4\sigma(F_o)$, 132 parameters, 0 restraints, $R1_{obsd.}$ = 0.106, $wR^2_{obsd.}$ = 0.298, $R1_{all}$ = 0.149, wR^2_{all} = 0.342, GOOF = 1.029, largest difference peak and hole: 0.662/−0.418 e·Å^{-3}.

Crystal Data for *Z*-3c:[37] $C_{18}H_{16}N_2$, *Mr* = 260.33 g·mol^{-1}, colourless prism, size 0.03 × 0.03 × 0.02 mm^3, orthorhombic, space group *Pca*2(1), *a* = 12.2813(5), *b* = 15.9945(8), *c* = 7.1037(3) Å, *V* = 1395.4(1) Å^3, *T* = −90 °C, *Z* = 4, $\rho_{calcd.}$ = 1.239 g·cm^{-3}, μ(Mo-K_α) = 0.73 cm^{-1}, *F*(000) = 552, 3032 reflections in *h*(−15/15), *k*(−20/20), *l*(−9/9), measured in the range 3.04° ≤ Θ ≤ 27.49°, completeness $\Theta_{max.}$ = 99.5%, 3032 independent reflections, 2000 reflections with $F_o > 4\sigma(F_o)$, 245 parameters, 1 restraints, $R1_{obsd.}$ = 0.0487, $wR^2_{obsd.}$ = 0.0894, $R1_{all}$ = 0.0981, wR^2_{all} = 0.1045, GOOF = 0.985, Flack-parameter 2(4), largest difference peak and hole: 0.146/−0.206 e·Å^{-3}.

Acknowledgments

Financial support by the Deutsche Forschungsgemeinschaft (Sonderforschungsbereich 436) and by the Thüringer Ministerium für Wissenschaft, Forschung und Kultur (Erfurt, Germany) is gratefully acknowledged. Moreover, we thank Dr. W. Günther (Jena) for his excellent advices in the course of our NMR investigations.

[1] [1a] H. Schiff, *Justus Liebigs Ann.* **1864**, *131*, 118.
[2] [2a] W. R. Layer, *Chem. Rev.* **1963**, *63*, *5*, 489−510.[2b] P. Y. Sollenberger, R. B. Martin, in *Chem. Amino Group* (Ed.: S. Patai), Interscience Publ., London, **1968**, 349−406.[2c] P. G. Taylor, in *Chemistry of the Double-Bonded Functional Groups* (Ed.: S. Patai), Wiley 1977−1997, Chichester, UK, **1997**, 3(2), 1103−1133.[2d] M. Bartok, G. Schneider, in *Chemistry of the Double-Bonded Functional Groups* (Ed.: S. Patai), Wiley 1977−1997, Chichester, UK, **1997**, 3(2), 1223−1251.[2e] D. J. Berger, J. M. Tanko in *Chemistry of the Double-Bonded Functional Groups* (Ed.: S. Patai), Wiley 1977−1997, Chichester, UK, **1997**, 3(2), 1281−1354.[2f] P. Hlavica, M. Lehnerer, in *Chemistry of the Double-Bonded Functional Groups* (Ed.: S. Patai), Wiley 1977−1997, Chichester, UK, **1997**, 3(2), 1625−1663.
[3] T. Abellan, R. Chinchilla, N. Galindo, G. Guillena, C. Najera, J. M. Sansano, *Eur. J. Org. Chem.* **2000**, 2689−2697 and references cited therein.
[4] G. Alvaro, D. Savoia, *Synlett* **2002**, *5*, 651−673.
[5] [5a] J. F. Larrow, E. N. Jacobsen, *J. Org. Chem.* **1994**, *59*, 1939−1942. [5b] S. E. Schaus, B. D. Brandes, J. F. Larrow, M. Tokunaga, K. B. Hansen, A. E. Gould, M. E. Furrow, E. N. Jacobsen, *J. Am. Chem. Soc.* **2002**, *124*, 1307−1315 and ref.[17] therein.
[6] M. E. Bluhm, M. Ciesielski, H. Görls, M. Döring, *Angew. Chem.* **2002**, *114*, 3104−3107; *Angew. Chem. Int. Ed.* **2002**, *41*, 0000−0000 !!!!!!!.
[7] [7a] D. J. Darensbourg, P. Rainey, J. Yarbrough, *Inorg. Chem.* **2001**, *40*, 986−993. [7b] D. J. Darensbourg, J. C. Yarbrough, *J. Am. Chem. Soc.* **2002**, *124*, 6335−6342.
[8] [8a] D. Walther, S. Geßler, U. Ritter, A. Schmidt, K. Hamza, W. Imhof, H. Görls, J. Sieler, *Chem. Ber.* **1995**, *128*, 281−287. [8b] D. Walther, U. Ritter, R. Kempe, J. Sieler, B. Undeutsch, *Chem. Ber.* **1992**, *125*, 1529−1536.
[9] [9a] M. Cheng, D. R. Moore, J. J. Reczek, B. M. Chamberlain, E. B. Lobkovsky, G. W. Coates, *J. Am. Chem. Soc.* **2001**, *123*, 8738−8749. [9b] B. M. Chamberlain, M. Cheng, D. R. Moore, T. M. Ovitt, E. B. Lobkovsky, G. W. Coates, *J. Am. Chem. Soc.* **2001**, *123*, 3229−3238.
[10] H. Hao, S. Bhandari, Y. Ding, H. W. Roesky, J. Magull, H.-G. Schmidt, M. Noltemeyer, C. Cui, *Eur. J. Inorg. Chem.* **2002**, 1060−1065.
[11] [11a] E. Lopez-Calle, M. Keller, W. Eberbach, *Eur. J. Org. Chem.* **2003**, *8*, 1438−1453. [11b] A. S. Gothelf, K. V. Gothelf, R. G. Hazell, K. A. Jørgensen, *Angew. Chem.* **2002**, *114*, 4410−4412. [11c] K. V. Gothelf, K. A. Jørgensen, *Chem. Rev.* **1998**, *98*, 863−909.
[12] [12a] A. E. Martell, *Acc. Chem. Res.* **1989**, *22*, 115−124 and references cited therein. [12b] M. D. Toney, *Biochemistry* **2001**, *40*, 1378−1384. [12c] B. Witkop, T. W. Beiler, *J. Am. Chem. Soc.* **1954**, *76*, 5589−5597. [12d] J. E. Dixon, T. C. Bruice, *Biochemistry* **1973**, *12*, 4762−4766. [12e] J. R. Maley, T. C. Bruice, *J. Am. Chem. Soc.* **1968**, *90*, 2843−2847. [12f] E. H. Abbott, M. E. Bobrick, *Biochemistry* **1973**, *12*, 846−851.
[13] [13a] E. Anders, *Synthesis* **1978**, *8*, 586−588. [13b] E. Anders, *Tetrahedron Lett.* **1978**, *38*, 3547−3548. [13c] W. Will, *Dissertation*, University of Erlangen-Nürnberg, **1982**. [13d] A. Stankowiak, *Dissertation*, University of Erlangen-Nürnberg, **1986**. [13e] A. Opitz, *Dissertation*, University of Erlangen-Nürnberg, **1992**. [13f]E. Anders, W. Will, A. Stankowiak, *Chem. Ber.* **1983**, *116*, 3192−3204. [13g] E. Anders, A. Stankowiak, *Synthesis* **1984**, 1039−1041. [13h] E. Anders, U. Korn, A. Stankowiak, *Chem. Ber.* **1989**, *122*, 105−111. [13i] R. Wagner, B. Wiedel, W. Günther, H. Görls, E. Anders, *Eur. J. Org. Chem.* **1999**, 2383−2390.
[14] S. Pawlenko, *Houben-Weyl: Methods of Organic Chemistry*, **1990**, vol. E 14b, part I, 222−281.
[15] [15a] H. Kessler, D. Leibfritz, *Chem. Ber.* **1971**, *104*, 2143−2157 and references cited therein. [15b] H. Kessler, D. Leibfritz, *Tetrahedron* **1970**, *26*, 1805−1820. [15c] H. Kessler, *Angew. Chem.* **1970**, *82*, 237−253.
[16] [16a] M. Raban, *J. Chem. Soc., Chem. Commun.* **1970**, 1415−1416. [16b] E. Carlson, F. B. Jones, Jr., M. Raban, *J. Chem. Soc., Chem. Commun.* **1969**, 1235−1237. [16c] N. P. Marullo, E. H. Wagener, *Tetrahedron Lett.* **1969**, *30*, 2555−2558. [16d] H.-J. Hofmann, T. Asano, R. Cimiraglia, R. Bonaccorsi, *Bull. Chem. Soc., Jpn.* **1993**, *66*, 130−134.
[17] [17a] C. Lambert, P. v. R. Schleyer, *Houben-Weyl: Methods of Organic Chemistry*, **1993**, vol. E 19d, 1−113. [17b] M. Schlosser, *Organometallics in Synthesis.A Manual*, 2nd ed., John Wiley & Sons, New York, **2002**, 1−352. [17c] L. Pauling, *The Nature of the Chemical Bond*, 3rd ed., Cornell University Press, Ithaca, New York, **1960**. [17d]T. Chan, I. Fleming, *Synthesis* **1979**, 761−786.
[18] S. O. Nilssonj Lill, U. Köhn, E. Anders, *Eur. J. Org. Chem.* **2004**, *13*, 2868−2880.
[19] J.-A. van den Berg, K. R. Seddon, *Chryst. Growth Design* **2003**, *3*, 643−661.
[20] Gaussian 98, Revision A-11; M. J. Frisch, G. W. Trucks, H. B. Schlegel, G. E. Scuseria, M. A. Robb, J. R. Cheeseman, V. G. Zakrzewski, J. A. Montgomery, R. E. Stratmann, J. C. Burant, S. Dapprich, J. M. Millam, A. D. Daniels, K. N. Kudin, M. C. Strain, O. Farkas, J. Tomasi, V. Barone, M. Cossi, R. Cammi, B. Mennucci, C. Pomelli, C. Adamo, S. Clifford, J. Ochterski, G. A. Petersson, P. Y. Ayala, Q. Cui, K. Morokuma, D. K. Malick, A. D. Rabuck, K. Raghavachari, J. B. Foresman, J. Cioslowski, J. V. Ortiz, B. B. Stefanov, G. Liu, L. A., P. P., I. Komaromi, R. Gomperts, R. L. Martin, D. J. Fox, T. Keith, M. A. Al-Laham, C. Y. Peng, A. Nanayakkara, C. Gonzalez, M. Challacombe, P. M. W. Gill, B. Johnson, W. Chen, M. W. Wong, J. L. Andres, C. Gonzalez, M. Head-Gordon, E. S. Replogle, J. A. Pople, *Gaussian, Inc.,* Pittsburgh PA, **1998**.
[21] [21a] A. E. Reed, L. A. Curtiss, F. Weinhold, *Chemical Reviews (Washington, DC, United States)* **1988**, *88*, 899−926. [21b] E. D. Gledening, A. E. Reed, J. E. Carpenter, F. Weinhold, *Natural Bond Orbital*, NBO 3.0 Program Manual, Theoretical Chemistry Institute and Department of Chemistry, University of Wisconsin, Madison, WI, **1988**.
[22] [22a] K. Wolinski, J. F. Hinton, P. Pulay, *J. Am. Chem. Soc.* **1990**, *112*, 8251−8260. [22b] R. Ditchfield, *Mol. Phys.* **1997**, *27*, 789−807. [22c] D. B. Chesnut, C. K. Foley, *Chem. Phys. Lett.* **1985**, *118*, 316−321.

[23] E. Anders, A. Opitz, N. J. R. van Eikema Hommes, F. Frankel, *J. Org. Chem.* **1993**, *58*, 4424−4430.
[24] [24a] A. Sygula, P. W. Rabideau, *J. Am. Chem. Soc.* **1992**, *114*, 821−824. [24b] M. Bühl, N. J. R. v. Eikema Hommes, P. v. R. Schleyer, U. Fleischer, W. Kutzelnigg, *J. Am. Chem. Soc.* **1991**, *113*, 2459−2465.
[25] [25a] P. S. Patterman, I. L. Karle, G. D. Stucky, *J. Am. Chem. Soc.* **1970**, *92*, 1150−1157. [25b] M. A. Beno, H. Hope, M. M. Olmstead, P. P. Power, *Organometallics* **1986**, *4*, 2117−2124. [25c] W. Zarges, M. Marsch, K. Harms, G. Boche, *Chem. Ber.* **1989**, *122*, 2303−2310. [25d] W. Zarges, M. Marsch, K. Harms, G. W. Frenking, G. Boche, *Chem. Ber.* **1991**, *124*, 543−549.
[26] [26a] J. Kaneti, P. v. R. Schleyer, T. Clark, A. Kos, G. W. Spitznagel, J. G. Andrade, J. B. Moffat, *J. Am. Chem. Soc.* **1986**, *104*, 1481−1492. [26b] R. Glaser, A. Streitwieser, *J. Org. Chem.* **1991**, *56*, 6612−6624.
[27] [27a] G. Wolf, E.-U. Würthwein, *Chem. Ber.* **1991**, *124*, 655−663. [27b] G. Wolf, E.-U. Würthwein, *Chem. Ber.* **1991**, *124*, 889−896.
[28] [28a] J. H. Gilchrist, A. T. Harrison, D. J. Fuller, D. B. Collum, *J. Am. Chem. Soc.* **1990**, *112*, 4069−4070. [28b] A. S. Galiano-Roth, E. M. Michaelides, D. B. Collum, *J. Am. Chem. Soc.* **1988**, *110*, 2658−2660. [28c] J. S. DePue, D. B. Collum, *J. Am. Chem. Soc.* **1988**, *110*, 5518−5524, 5524−5533.
[29] For related experimental and theoretical studies see: [29a] M. Piffl, J. Weston, E. Anders, *Eur. J. Org. Chem.* **2000**, 2851−2859. [29b] M. Bräuer, J. Weston, E. Anders, *J. Org. Chem.* **2000**, *65*, 1193−1199. [29c] A. Opitz, R. Koch, A. R. Katritzky, W. Fan, E. Anders, *J. Org. Chem.* **1995**, *60*, 3743−3749.
[30] [30a] P. J. Taylor, *J. Chem. Soc., Perkin Trans. 2* **1972**, 1077−1086. [30b] R. G. Button, P. J. Taylor, *J. Chem. Soc., Perkin Trans. 2* **1973**, 557−567.
[31] [31a] H. Benhaoua, F. Texier, R. Carrie, *Tetrahedron* **1986**, *42*, 2283−2291. [31b] R. Huisgen, *Angew. Chem.* **1963**, *75*, 604−637.
[32] S. J. Storfer, E. I. Becker, *J. Org. Chem.* **1962**, *27*, 1868−1876.
[33] COLLECT, Data Collection Software; Nonius B.V., Netherlands, **1998**.
[34] Z. Otwinowski, W. Minor, "Processing of X-ray Diffraction Data Collected in Oscillation Mode", in *Methods in Enzymology*, vol. 276, Macromolecular Crystallography, Part A (Eds.:C. W. Carter, R. M. Sweet), pp. 307−326, Academic Press, **1997**.
[35] G. M. Sheldrick, *Acta Crystallogr., Sect. A* **1990**, *46*, 467−473.
[36] G. M. Sheldrick, SHELXL-97, University of Göttingen, Germany, **1997**.
[37] CCDC-238419 (for **[4e(THF)$_2$I$_2$]**) and -238420 (for **Z-3c**) contains the supplementary crystallographic data for this paper. These data can be obtained free of charge via www.ccdc.cam.ac.uk/conts/retrieving.html (or from the Cambridge Crystallographic Data Centre, 12 Union Road, Cambridge CB2 1EZ, UK; Fax: + 44-1223-336-033; or deposit@ccdc.cam.ac.uk).
Received July 1, 2004

